TRABAJO ESPECIAL DE GRADO

ANÁLISIS DE REGISTROS DE POZO, Y ESTIMACIÓN DE LAS PROPIEDADES GEOMECÁNICAS E HIDRÁULICAS A TRAVÉS DEL USO DE LA ECUACIÓN DE GASSMANN.

ANALYSIS OF BOREHOLE DATA (LOGS), AND ESTIMATION OF GEOMECHANICAL AND HYDRAULIC PROPERTIES USING GASSMANN'S EQUATION.

Presentado ante la Ilustre

Universidad Central de Venezuela

Por el Br. Jeshua Guzmán.

Para optar al título de Ingeniero Geofísico

Caracas, Noviembre 2014

TRABAJO ESPECIAL DE GRADO

ANÁLISIS DE REGISTROS DE POZO, Y ESTIMACIÓN DE LAS PROPIEDADES GEOMECÁNICAS E HIDRÁULICAS A TRAVÉS DEL USO DE LA ECUACIÓN DE GASSMANN.

ANALYSIS OF BOREHOLE DATA (LOGS), AND ESTIMATION OF GEOMECHANICAL AND HYDRAULIC PROPERTIES USING GASSMANN'S EQUATION.

TUTORES ACADÉMICOS:

Prof. Alberto Godio (Politécnico de Turín)

Prof. Antonio Ughi.

Presentado ante la Ilustre

Universidad Central de Venezuela

Por el Br. Jeshua Guzmán.

Para optar al título de Ingeniero Geofísico

Caracas, Noviembre 2014

COTA: TESIS 2014-11

Guzmán C., Jeshua D.

ANALYSIS OF BOREHOLE DATA (LOGS), AND ESTIMATION OF GEOMECHANICAL AND HYDRAULIC PROPERTIES USING GASSMANN'S EQUATION.

Prof. Guía: Alberto Godio. Tesis. Caracas. UCV. Facultad de Ingeniería. Escuela de Geología, Minas y Geofísica. Ingeniero Geofísico. Institución: Politecnico di Torion. 2014.

Palabras Claves: Ecuación de Gassmann, Petrofísica, Registros de pozos (Logs), Algoritmo Matlab, Propiedades geomecánicas, Propiedades hidráulicas, Sustitución de fluidos.

Resumen: La sustitución de fluidos de Gassmann es esencial para estimar el comportamiento de fluidos en condiciones de yacimiento, así como para llevar a cabo el análisis de los datos de pozos en la presencia de dos o más fluidos. Además, proporciona las herramientas necesarias para identificar y cuantificar los fluidos del yacimiento. Este estudio se presentará en dos fases principales, la primera de ellas destaca el análisis de los datos del pozo (logs). Los datos fueron obtenidos de una base de dato científica (en concreto de Darling, 2005), donde se analizó un yacimiento con una profundidad entre 2020ft y 2214ft, el mismo fue subdivido en 4 zonas prospectivas de acuerdo al contenido de fluidos y litología. En la segunda fase, se ejecutó un algoritmo implementado en Matlab, el mismo fue adaptado para estimar las principales propiedades y parámetros geomecánicos e hidráulicos de la roca a través del uso de la ecuación de Gassmann. Este se aplicó específicamente entre 2042ft y 2120ft (zona 2).

Abstract

In the analysis of sonic and acoustic logs, Gassmann's fluid substitution is essential for estimating fluid behaviour under reservoir conditions, as well as performing the analysis of well data in the presence of two or more fluids. Also, it provides the necessary tools to identify and quantify reservoir fluids.

This study will be presented in two main phases, the first one highlights the analysis of borehole data (logs); data was given in scientific database (specifically Darling, 2005) where a reservoir with a depth between 2020ft and 2214ft was analyzed and divided into 4 zones. In the second phase, a systematic algorithm of Gassmann's equation has been implemented in Matlab and adapted to estimate the main geomechanical and hydraulic parameters of rock. This was applied specifically between 2042ft and 2120ft (zone 2).

In the first phase, a quality control was performed in order to identify outliers, as well as to verify the datum and deviated well corrections. After that, it proceeded to identify the hydrocarbon reservoir through Gamma Ray and Neutron Density Logs. Subsequently, the fluid type and present contacts were identified using resistivity log, sonic, and pressure gradients. Thus, the integrated analysis of these results allows one to infer the total porosity ($Ø_{total}$), hydrocarbon saturations (S_{hyd}) and acoustic impedances (AI). Finally, through the integration of the results, it was possible to divide the reservoir into 4 zones, and identify the most prospective area.

The second phase was based on the implementation of Gassmann's equation in zone 2. This was performed by carrying out an analysis before and after fluid replacement (From Oil to Brine/Gas) took place. It was possible to identify significant changes in density and acoustic impedances, as well as helping to identify lithological interfaces and improve understating of the fluids behaviour in the reservoir.

Acknowledgements

First and foremost I would like to thank my mother, Maribel Castro, and my Aunt Jackeline Castro, for providing me with the strength and courage to successfully carry out my ambitions and follow my dreams. Without their continual love and support I would not be where I am today. Although, unfortunately they are not able to be here with me for my graduation, they will always have a special place in my heart. Thank you for believing in me when no one else did, your selflessness has truly made all the difference.

To my advisor Alberto Godio, thank you for giving me the opportunity to expand my knowledge in the field of petrophysics, by using your technical and scientific awareness in order to assist me with the development of my thesis.

I wish to express my thanks to Megan Herbert, who, with her love and daily unconditional support has helped me during the most difficult and crucial moments in the development of my thesis. Even when no one else was, she was there to motivate and encourage me, thank you for your patience.

I would like to give special thanks to my professors in Venezuela, whose perseverance and dedication has formed the technical and scientific foundation which has enabled me to further my studies and will surely assist me in every step of my future career.

I would especially like to thank my professor of seismic processing Vincenzo De Lisa, for helping me get onto the double degree agreement programme.

I would like to give huge thanks to my friends here in Turin, particularly to Robert Spanna, José Quintero Lehmann and Leidy Carolina Centeno, for helping me in some crucial stages in the development of my thesis, and for providing me with countless fun times and memories which will last a life time.

Last but not least I would like to thank all of my family and friends who have helped me either before, and or during my time here in Turin, your kind wishes have not gone unnoticed, I appreciate each and every one of you, thank you all.

Table of Contents

1 Introduction

The role played by a petrophysicist in the oil industry is without a doubt one of the most important with regards to the analysis and identification of a hydrocarbon reservoir. When working together, petro physicists and Reservoir engineers can provide important information to facilitate the estimation of mechanical and hydraulic rock properties. Such information is obtained through the analysis and study of borehole data logs in order to create a static and dynamic model. These models provide information concerning the fluids behaviour at reservoir conditions, and help predict key parameters governing the reservoir, such as hydrocarbon saturations, densities, porosities, permeabilities, among others. For that reason, it is necessary that the parameters obtained through a petrophysical study are as accurate as possible.

One of the most useful tools for a petrophysicist is Gassmann's equation, as it relates directly to the Bulk modulus of the rock matrix (K_{matrix}) and the Rock frame with the porous media, as well as the present fluid properties. In order to better understand this terminology, outlined below is an annotated diagram (figure 1) which describes the following four major factors:

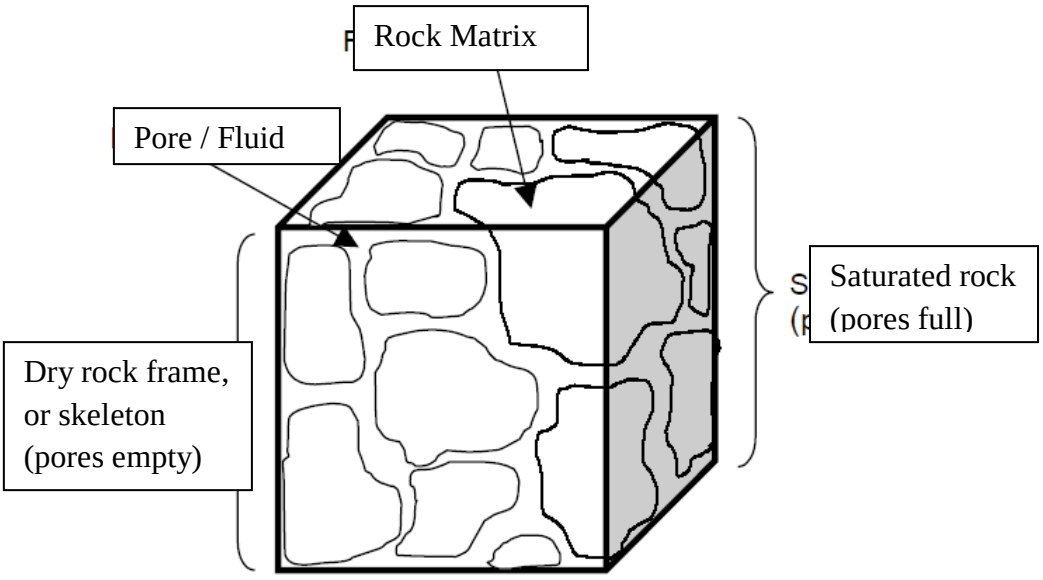

Figure 1: Illustration of the key characteristics that form the basis for understanding the Biot-Gassmann theory. (Brian H. Russell et al, 2001)

There are several theories concerning the physics of rocks, however, the fluid substitution model using Gassmann's equation is one of the most important. Gassmann's theory is useful for estimating densities, P and S wave velocities when fluid saturations increase or decrease at different rates.

On the other hand, the constraints and assumptions of this theory have been studied and analyzed over the last 60 years since Gassmann and Biot published their theory in 1951 and 1956 respectively. Gasmann's theory has mainly been applied to the distribution of low frequency waves, while Biot's theory derived an expression that also includes high frequencies. However, this theory assumes a homogeneous, isotropic and inelastic medium, as well as high effective porosity. It also assumes that there is no fluid exchange between boundaries or chemical reactions with each other.

In recent years diverse studies have been conducted. These studies are related to the use of the Biot-Gassmann equation in order to improve the recovery factor in the reservoir, and at the same time, to accurately estimate the main hydraulic and geomechanical parameters of rocks in reservoir conditions.

Among the most relevant authors who have helped the development and understanding of this theory we find Han, (1992), Mavko et al. (1995), Berryman (1999).

The overall objective of this study is to perform an analysis of borehole data logs in an oil reservoir, in order to identify important reservoir parameters such as porosities, densities, shale volumes, water saturations, among others. These data are required in order to apply the Biot-Gassmann theory through a mathematical algorithm implemented in Matlab. Therefore, I intend to create a model of density and seismic wave velocities, before and after implementing Gassmann's fluid substitution, and will proceed to analyze the main variations.

In Table 1 the necessary input for fluid replacement through Matlab is listed, as well as the reference values in an oilfield.

Table 1: input required to perform Gassmann's fluid replacement.

Matlab Imput	Values	Unit	Reference range
Oil Gravity	35	API	30 < light oil < 40 API
GOR	100	l/l	
Gas Gravity	0.7	API	0.6-0.9 Api
Salinity	10000	ppm	2000 - 270000 ppm (10000ppm = 1%)
TWS, Target Sw	1	fraction	
Temperature	100	º C	50 – 200 ºC
Porosity	From logs	fraction	0.1-0.3
Pression	From logs	Psia	3000 - 6000
Vp	From logs	ft/s	11000 - 16000 (3500 - 5500 m/s)
Vs	From logs	ft/s	3000 - 11500 (930 - 3500 m/s)
Density	From logs	g/cc	2.3 - 2.6
Vsh	From logs	fraction	0 - 1
Inicial Sw	From logs	fraction	Siw - 1

As far as the methodology is concerned, this study was divided into two main phases. The first phase consisted of the reservoir and fluid identification, as well as the quantification of fluids in the study area. Instead, the second phase was based on the implementation of the Biot-Gassmann equation in Matlab. The following diagram briefly illustrates how this study was conducted:

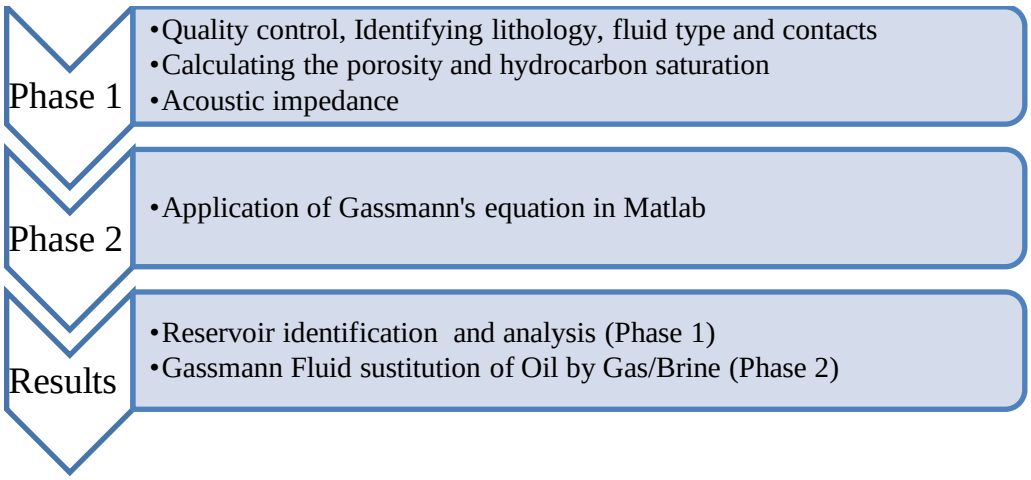

Figure 2: Overview of Diagram of the methodology applied

2 Background and fundamental theory on analysis of borehole data

2.1 Petrophysical properties

Well logs are commonly used to obtain the hydraulic and mechanical properties of a rock. These properties are known as elastic constants of rocks, such as the bulk modulus, Young's Modulus, shear modulus, and Poisson's Ratio. The dynamic elastic constants can be estimated by using suitable equations such as density log data, shear travel time and sonic log compressional.

The nature of reservoir rocks containing gas and oil indicates the amount of fluid trapped in the void spaces of these rocks, in addition to the ability of these fluids to flow through rocks and other related physical properties. The measurement of the empty space is known as porosity of the rock, and the measurement of the capability of the rock to transmit fluid is called permeability. Knowledge of these two hydraulic properties is essential before questions concerning types of fluid, amount of fluid, rates of fluid flow, and fluid recovery estimates can be answered. Methods of measuring porosity and permeability comprise much of the technical theory of the oil industry. Hydraulic properties can be obtained from laboratory work and field estimation. Nevertheless, those techniques are limited in terms of time consumption and economy. (Djebbar, 2012). An overview of the mechanical and hydraulic properties of rocks is described below:

2.1.1 Mechanical properties

Elastic Moduli and Elastic Wave Velocities

The theory of elasticity gives the basis for the description of elastic wave propagation. Hooke's law describes the relationship between stress and strain of an elastic material. In a general formulation, the stress-strain relationship is a tensorial equation:

$$\boldsymbol{\sigma}_{ik} = \boldsymbol{C}_{iklm}.\boldsymbol{\varepsilon}_{lm} \quad (1)$$

Where, σik is the stress tensor, εlm is the strain tensor, Ciklm is the elastic modulus (or stiffness) tensor. For an isotropic material, the number of independent constants is reduced to two and the tensor of elasticity has takes the following form: (J.H. Schön, 2011)

$$\begin{bmatrix} C11 & C12 & C12 & 0 & 0 & 0 \\ C12 & C11 & C12 & 0 & 0 & 0 \\ C12 & C12 & C11 & 0 & 0 & 0 \\ 0 & 0 & 0 & C44 & 0 & 0 \\ 0 & 0 & 0 & 0 & C44 & 0 \\ 0 & 0 & 0 & 0 & 0 & C44 \end{bmatrix}$$

With $C_{12} = C_{11} - 2C_{44}$

The relationship between the components and the Lame parameters λ,μ are:

$$C_{11} = \lambda + 2\mu \qquad C_{12} = \lambda \qquad C_{44} = \mu$$

- As well as the Lame parameters λ,μ, any pair of two of the following moduli can be used for a description of the elastic properties of an isotropic material
- Young's modulus E, defined as ratio of stress to strain in a uniaxial stress state;
- Compressional wave modulus M, defined as ratio of stress to strain in a uniaxial strain state;
- Bulk compressional modulus k, defined as ratio of hydrostatic stress to volumetric strain1;
- Shear modulus μ, defined as ratio of shear stress to shear strain;
- Poisson's ratio v, defined as the (negative) ratio of lateral strain to axial strain in a uniaxial stress state.

Corresponding to the two moduli are two autonomous body waves, compressional, longitudinal, or P-wave with the velocity:

$$Vp = \sqrt{\frac{M}{\rho}} = \sqrt{\frac{E}{\rho}\frac{1-v}{(1-v)(1-2v)}} = \sqrt{\frac{K+(4/3)\cdot\mu}{\rho}} \qquad (2)$$

Shear, transversal, or S-wave with the velocity:

$$Vs = \sqrt{\frac{\mu}{\rho}} = \sqrt{\frac{E}{\rho}\frac{1}{2v\,(1+v)}} \qquad (3)$$

Where ρ is the bulk density.

In seismic and formation evaluation practice, the inverse of the velocity—the "slowness"—is frequently used (J.H. Schön, 2011):

- Compressional wave slowness Δt_p = DTP = V_p^{-1}
- Shear wave slowness Δt_s = DTS = Vs^{-1}

The ratio of the two wave velocities is only controlled by Poisson's ratio.

$$\frac{Vp}{Vs} = \sqrt{2\,\frac{1-v}{1-2v}} \tag{4}$$

For the minimum value of Poisson's ratio ν = 0 in a homogeneous, isotropic material, the minimum ratio is $V_P/V_S = \sqrt{2} \sim 1.4$ (see figure 3) thus, for real isotropic rocks, $V_P/V_S > \sqrt{2}$

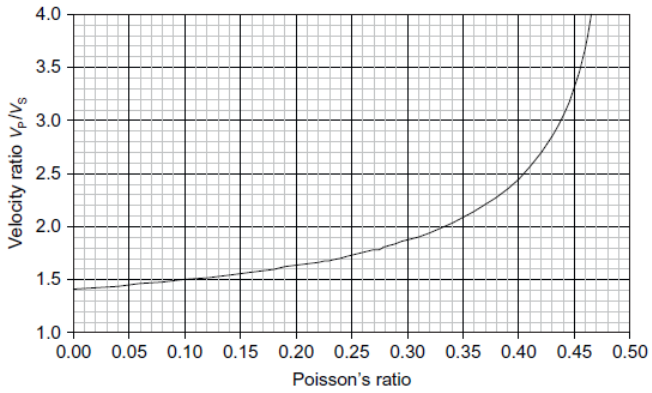

Figure 3: Velocity ratio vs Poisson ratio

However, if elastic wave velocities and bulk density are identified from the measurements, the elastic parameters can be calculated as follows: (J.H. Schön, 2011)

$$\mu = \rho \cdot V_s^2 \tag{5}$$

$$M = \rho \cdot V_P^2 \tag{6}$$

$$E = \rho\, V_P^2\, \frac{(1+v)(1-2v)}{1-v} \tag{7}$$

$$\lambda = \rho\, (V_P^2 - 2\, V_S^2) \tag{8}$$

$$k = \rho\, (V_P^2 - \frac{4}{3}\, V_S^2) \tag{9}$$

Elastic properties of the rocks constituents

a) Overview

Elastic properties of rocks are dominated by the properties of the solid rock skeleton including "defects" like pores, fractures, and cracks. In most cases, these defects have dimensions which are smaller than the wavelength.

The simplified drawing in Figure 4 illustrates the general tendencies for the basic rock components:

- Solid minerals: minerals, matrix components
- Fluids: liquids (water, oil), air, gas.

For compressional wave velocities: $V_{p,minerals} > V_{p,water,oil} > V_{p,gas}$ and for the corresponding compressional modulus: $k_{minerals} > k_{water,oil.kgas}$.

The shear modulus shows a completely different behavior, because by definition, fluids do not have a shear resistance ($\mu_{fluids} = 0$). Therefore, the density term of shear wave velocity shows only a minor dependence on pore fluids. (J.H. Schön, 2011).

Hence, the result of the following tendencies:

- Increasing porosity decreases both compressional and shear wave velocities;
- Compressional wave velocity is controlled also by the type of pore fluid (gas, liquid);
- Shear wave velocity is not strongly controlled by type of pore fluid.

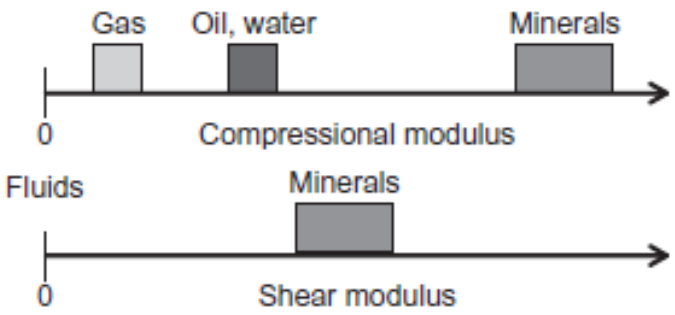

Figure 4: Compressional and shear modulus for main rock components. (J.H. Schön, 2011).

b) Solid Components, Minerals

There are several books where it is possible to find the magnitude of wave velocities and parameters of some rock-forming minerals, such as J.H. Schön, (2011) and Mavko (1998).

This was taken into consideration as a consequence of the following points:

- The composition of igneous rocks: that acid or felsic components have lower elastic moduli and velocities than basic or mafic components.
- The composition of reservoir rocks: that there is a significant difference between the three basic types of matrix substances quartz, calcite, and dolomite.

c) Fluids

Pore fluids, (gas, oil, and water) usually have distinct ranges of compressional or bulk modulus (shear modulus of fluids is zero). For point of reference, the following ranges are given for compressional bulk modulus k_{fluid} and density:

ρ_{fluid}:

Gas: $k_{fluid} \sim 0.01 - 0.4$ GPa $\quad \rho_{fluid} \sim 0.1 - 0.5 \cdot 10^3$ kg m^{-3}

Oil: $k_{fluid} \sim 0.4 - 3.0$ GPa $\quad \rho_{fluid} \sim 0.7 - 1.1 \cdot 10^3$ kg m^{-3}

Water: $k_{fluid} \sim 2.0 - 4.0$ GPa $\quad \rho_{fluid} \sim 0.9 - 1.2 \cdot 10^3$ kg m^{-3}

Appendix A (compressional wave velocity for some fluids).

Gas

Wang (2001) claims that ‘because most gases are extremely compressible under reservoir conditions, in many cases the bulk modulus (incompressibility) of a hydrocarbon gas can be set as 0.01 - 0.2 GPa in seismic modelling. Errors in gas bulk modulus will yield little uncertainty in the calculated seismic properties in a fluid-saturated rock.

Density of gas and Bulk modulus in a reservoir depend on temperature, pressure, and gas composition (Table 2).

Table 2: Some Value for Hydrocarbon Gas Density and Compressional Modulus *(Derived from the relationship (plot) by Batzle and Wang (1992), and calculated compressional wave velocities).*

Pressure and Temperature	**P in 103 kg m^{-3}**	**k in MPa**	**VP in m s^{-1}**
T = 373 ^{o} K (100 ^{o} C) p = 25 Mpa	0.150-0.35	50-150	550-650
T = 373 ^{o} K (100 ^{o} C) p = 50 Mpa	0.250-0.45	150-350	750-900
T = 473 ^{o} K (200 ^{o} C) p = 25 Mpa	0.120-0.30	50-80	500-600
T = 473 ^{o} K (200 ^{o} C) p = 50 MPa	0.200-0.40	130-200	550-650

Oil

A relationship published by Batzle and Wang (1992), describes the dependence of oil velocity (m/s) on API number, temperature T (ºC), and pressure p (MPa):

$$V_p = 15450(77.1 + API)^{-0.5} - 3.7 \cdot T + 4.64 \cdot p + 0.0115\,(0.36\,API^{0.5} - 1)\,T \cdot p \quad (10)$$

Table 3 shows some data based on the empirical equations from Batzle and Wang (1992).

Table 3: Some Value for Light Oil (50 API) Density and Compressional Modulus *(Derived from the relationship (plot) by Batzle and Wang (1992), and derived velocities).*

Pressure and Temperature	**ρ in 10^{3} kg m^{-3}**	**k in MPa**	**VP in m s^{-1}**
Dead oil, T = 373K (100C); p = 25 MPa	0.76	1100	1200
Dead oil, T = 473K (200C); p = 50 MPa	0.7	800	1070

Brine

Brine constitution can be obtained from water to saturated saline solution. Bulk modulus, density, and velocity of brine are controlled by a vast range of concentration, temperature, and pressure. In addition, Batzle and Wang (1992) acquired empirical equations and plots for the practical application of these relationships. Table 4 shows some selected data.

Table 4 Some Value for Brine Density and Compressional Modulus *(Derived from the relationship (plot) by Batzle and Wang (1992), and derived velocities).*

Concentration (Salinity), Pressure and Temperature	ρ in 10^3 kg m^{-3}	k in MPa	VP in m s^{-1}
Water, fresh, room conditions	1	2200	1480
Brine, 3.5 % salinity, room conditions	1.05	2400	1510
Brine T 5 373K (100C); p 5 25 Mpa	0.97	2600	1635
Brine T 5 473K (200C); p 5 50 MPa	0.9	2100	1530

2.1.2 Hydraulic properties

Porosity

The grains and particles of carbonate materials that make up sandstone and limestone reservoirs generally never fit together ideally due to the high degree of anomaly in the shape. This can be expressed in following mathematical equation as: (Djebbar Tiab, et al 2012).

$$\phi = \frac{Vp - Vgr}{Vp} = \frac{Vp}{Vb} \qquad (11)$$

Where:

$\emptyset$ = Porosity, fraction

V_b = Bulk volume of the reservoir rock

V_{gr} = Grain volume

V_p = Pore volume

In accordance with the porosity definition, the porosity of most sedimentary rocks is usually lower than 50%. (Djebbar Tiab, et al 2012).

Factors governing the magnitude of porosity

In an effort to determine approximate limits of porosity values, Fraser and Graton determined the porosity of various packing arrangements of uniform spheres as shown in Figure 5.

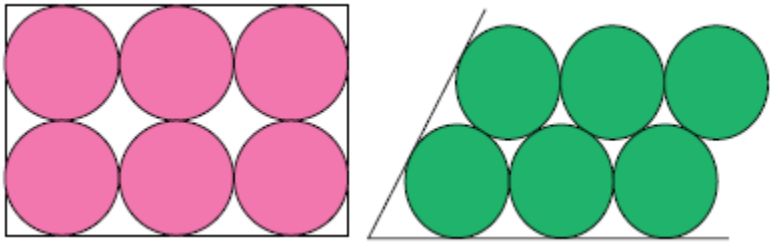

Figure 5: Cubic (left) and rhombohedral (right) packing of spherical grains.

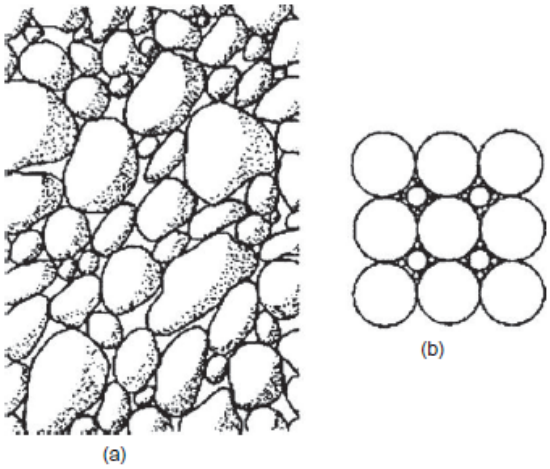

Figure 6: Collection of (a) different sized and shaped sand grains and (b) spheres illustrating a cubic packing of three grain sizes. Cubic (left) and rhombohedral (right) packing of spherical grains.

They have shown that the cubic, or wide-packed system, has a porosity of 47.6% and the rhombohedral, or close-packed system, has a porosity of 25.9%. The porosity for a system like this is independent of the grain size (sphere diameter). However, if smaller spheres are mixed among the spheres of either system, the ratio of pore space to the solid framework becomes lower, and porosity is reduced. (Gatlin C. 1960) Figure 6 (b) shows a three-grain-size cubic packing. The porosity of this cubic packing is now approximately 26.5%.

The porosities of petroleum reservoirs range from 5% to 30%, but most frequently are between 10% and 20%. Any porosity less than 5% is rarely profitable, and any porosity more than 35% is extremely unusual. The following table defines what typically constitutes poor, good, and very good levels of porosity. (Djebbar Tiab, et al 2012).

Fluid Saturation

The porosity of a reservoir rock is very important because it demonstrates the rock's ability to store fluids (oil, gas, and water). Equally important is the relative extent to which the rock's pores are filled with specific fluids. This property is called fluid saturation and is shown as a percentage, of the total pore volume occupied by oil, gas, or water. Thus, for instance, the oil saturation So is equal to:

$$So = \frac{Volume\ of\ oil\ in\ the\ rock, Vo}{\text{Total pore volume of the rock, Vp}} \tag{12}$$

Similar expressions can be written for gas and water. It is evident that:

$$S_o + S_g + S_w = 1 \tag{13}$$

and

$$V_o + V_g + V_w = V_p \tag{14}$$

Ideally, due to the difference in fluid densities, a petroleum reservoir is formed in such a way that there will be gas, oil, and water from the top to the bottom of the sand bed. This is shown in Figure 7 (Djebbar Tiab, et al. 2012).

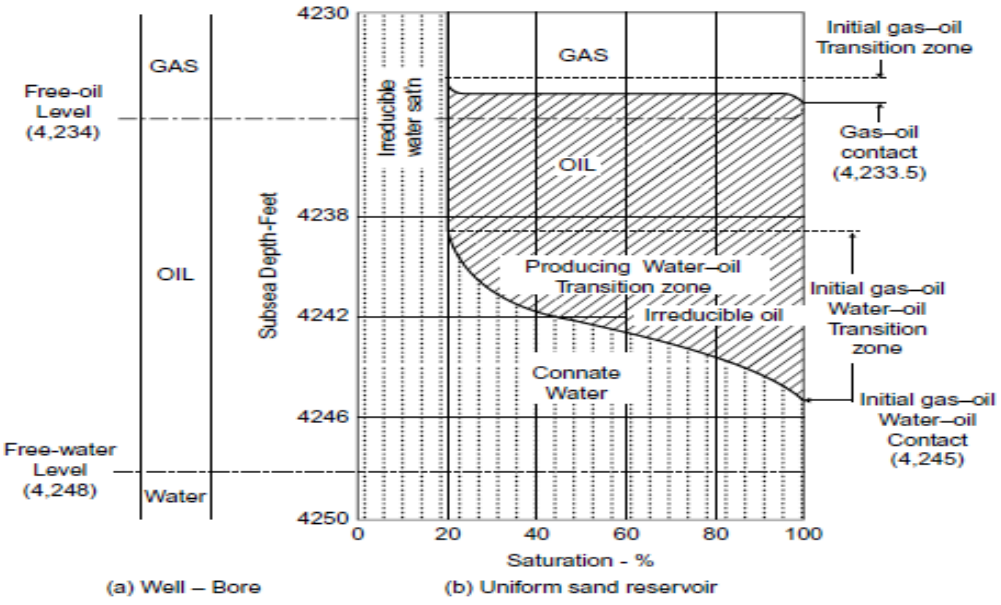

Figure 7: Distribution of fluids in reservoirs.

Permeability

As well as being porous, a reservoir rock must have the ability to allow petroleum fluids to flow through its interconnected pores. The rock's ability to conduct fluids is termed as permeability. This suggests that non-porous rocks have no permeability. The permeability of the rock is related with its porosity. Therefore, this is affected by the rock's grain size, grain packing, grain size distribution (sorting), grain shape, and the degree of cementation and consolidation. Likewise, the type of cementing material or clay between sand grains also impact on permeability, especially where fresh water is present. (Djebbar Tiab, et al 2012).

Some types of clay, particularly smectites (bentonites) and montmorillonites, swell in fresh water and have a tendency to completely or partially block the pore spaces.

In 1856, a French engineer called Henry Darcy developed a fluid flow equation that has since become one of the standard mathematical tools frequently used by petroleum engineers (Darcy HJ, 1856). This equation, (which is used to measure the permeability of a core sample as shown in Figure 8), is expressed in differential form as follows:

$$V = \frac{q}{Ac} = -\frac{K}{\mu}\frac{dp}{dl} \qquad (15)$$

Where:

V = velocity of fluid, cm/s

q = Rate, cm^3/s

K = permeability, Darcy (0.986923 μm^2)

Ac = core cross area,, cm^2

μ = viscosity of the fluid, centipoises (cP)

l = length of the core sample, cm

dp/dl = pressure gradient (atm/cm)

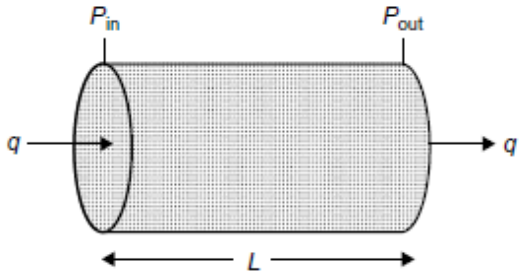

Figure 8: Core Sample

One darcy indicates a relatively high level of permeability. The permeability of mo stpetroleum reservoir rocks is less than one darcy. Hence why, a smaller unit of permeability, such as the millidarcy (mD), is widely used in the oil and gas industry. In SI units, the square micrometer (μm^2) is used instead of m^2.

In the case of more than one fluid, permeability is called the "effective" permeability (ko, k_g, or k_w being oil, gas, or water effective permeability, respectively). Reservoir fluids interface with each other during their movement through the porous channels of the rock. Consequently, the sum of the effective permeabilities of all the phases will always be less than the absolute permeability. (Djebbar Tiab, et al 2012).

Classification of Permeability

Petroleum reservoirs can have primary permeability, (also known as the matrix permeability) and secondary permeability. Matrix permeability occurs during the period of lithification and deposition (hardening) of sedimentary rocks. Secondary permeability results from the alteration of the rock matrix by compaction, cementation, fracturing, and solution.

Whereas compaction and cementation generally reduce the permeability, (as shown in Figure 9) fracturing and solution tend to increase it (Clark NJ, 1969). In some reservoir rocks, (particularly low-porosity carbonates) secondary permeability provides the main flow conduit for fluid migration, e.g. the Ellenburger Field, TX.

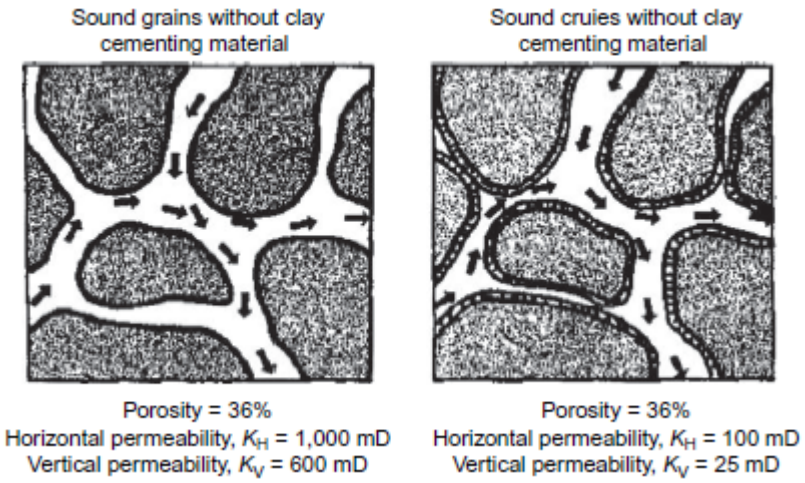

Figure 9: Effects of clay cementing material on porosity and permeability (Clark NJ, 1969).

Factors affecting the magnitude of permeability

Permeability of petroleum reservoir rocks can range from 0.1 to 1,000 or more millidarcies. The quality of a reservoir determined by permeability in mD, can be judged as: poor if k < 1, fair if 1 < k < 10, moderate if 10 < k <50, good if 50 < k <250, and very good if k > 250 mD. (Djebbar Tiab, et al 2012).

Reservoirs which have a level of permeability below 1 mD are considered “tight.” Factors affecting the magnitude of permeability in sediments are as follows:

- Shape and size of sand grains: If the rock is composed of large and flat grains uniformly arranged with the longest dimension horizontal, (illustrated in Figure 10) its horizontal permeability (k_H) will be very high, whereas vertical permeability (k_V) will be medium-to-large. If the rock is composed of mostly large and rounded grains, its permeability will be considerably higher and of the same magnitude in both directions (shown in Figure 10b). Permeability of reservoir rocks is generally low, especially in the vertical direction, and if the sand grains are small and of irregular shape (Figure 10c). Most petroleum reservoirs fall into this category. Reservoirs with directional permeability are called anisotropic reservoirs. Anisotropy greatly affects fluid flow characteristics of the rock (Djebbar Tiab, et al 2012).

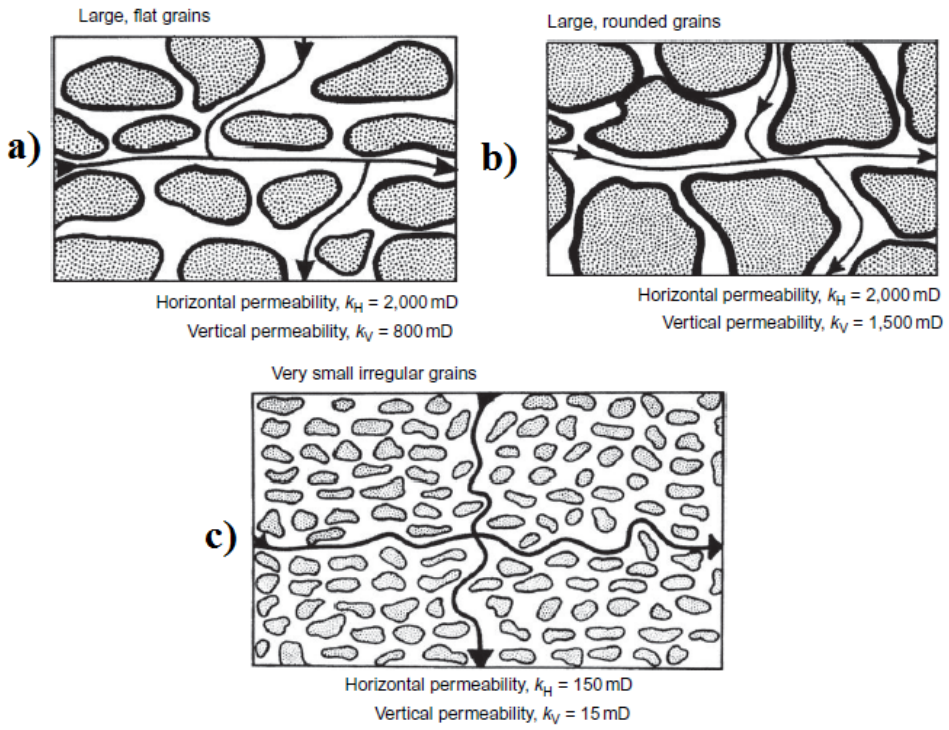

Figure 10: a) Effects of large flat grains on permeability, b) Effects of large rounded grains on permeability, c) Effects of small, irregular grains on permeability (Clark NJ, 1969).

2.2 Analysis of relationships between petrophysical properties and seismic attribute

The Gassmann model (Gassmann, 1951) estimates the elastic properties of a porous rock at one fluid state, and predicts the properties for another fluid state. Thus, it allows a "fluid substitution" or "fluid replacement." This fluid substitution is an important part of the seismic rock physical analysis, which relates seismic velocities to the rocks' elastic properties. In the theoretical world, many tutorial theses about technical theory have been published. An example of this is Kumar (2006), who has given a lecture in accordance with a program from MATLAB.

2.2.1 Gassmann's Static Model

Gassmann (1951) developed a model for porous rocks which enable the prediction of velocities if rocks are saturated with one fluid (e.g., water) from velocities if rocks are saturated with a different second fluid (e.g., gas) and vice versa (J.H. Schön, 2011).

Gassmann's theory assumes (Dewar and Pickford, 2001) the following:

- The rock is macroscopically homogeneous and isotropic: This assumption ensures that wavelength > grain and pore size (this is given in most cases of seismic field and laboratory measurements). The statistical isotropic porous material with homogeneous mineral moduli makes no assumptions with respect to any pore geometry.
- Within the interconnected pores, there is a fluid pressure equilibrium and no-pore pressure gradient as a result of passing waves. Thus, the low frequency allows a balance between the pore pressure within the pore space. Therefore, Gassmann's equation works best for seismic frequencies (<100 Hz) and high permeability (Mavko et al., 1998).
- Pores are filled with non-viscous, frictionless fluids. This also contributes to pore pressure equilibrium which results in a fluid independent shear modulus of the porous rock.
- The rock-fluid system is closed (un-drained), that is, no fluid can flow in or out of the specified volume during wave passage.
- The pore fluid does not is associated with any the solid material or rock frame. Gassmann's model does not implement any change of the "rock skeleton or frame modulus" by changing fluids (e.g., softening in case of swelling clay cement by replacement of oil by water with reactive chemical composition or in general as a result of changing surface energy).
- A passing wave results in the motion (displacement) of the entire rock section, but there is no relative motion between solid rock skeleton and fluid. The exact amount is given only for zero frequency (static solution). For high frequencies, a relative motion can result in dispersion.

Changing pore fluid influences velocity of elastic waves as a result of changing elastic moduli and changing density. The effects can be described as follows: (J.H. Schön, 2011)

1. Density follows the equation:

$$\rho = (1- \emptyset) \cdot \rho_s + \emptyset \cdot \rho_{fl} \tag{16}$$

2. Shear modulus is independent on the fluid type

$$\mu_{dry} = \mu_{sat} = \mu \tag{17}$$

3. Compressional bulk modulus is strongly dependent on fluid compressional modulus and the key parameter in Gassmann's model. Figure 11 explains the theory of origin for the two cases.

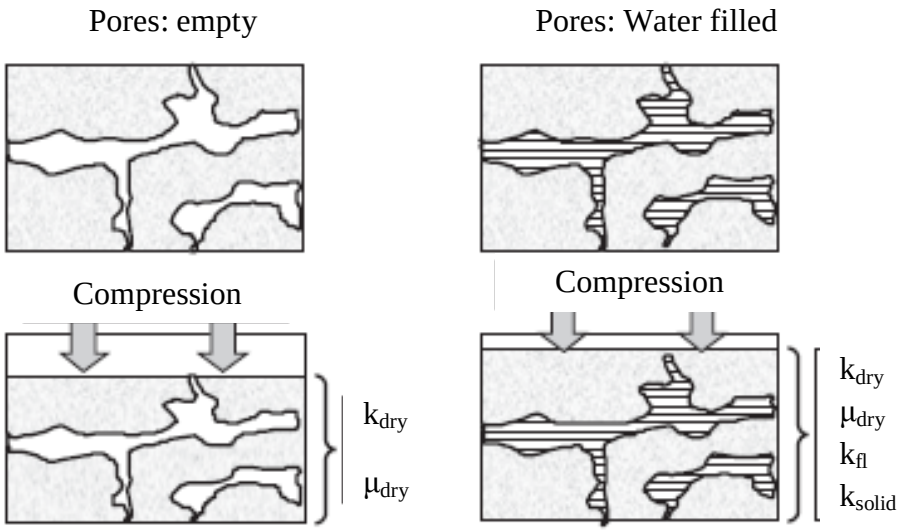

Figure 11: Derivation of Gassmann's equation. Left side: dry porous rock under the influence of a compression. Right side: fluid-saturated porous rock under the influence of a compression.

The left side describes the "dry case": the pores are empty and so, pore fluid has zero bulk modulus and does not contribute to the compression resistance (pore fluid also has zero shear modulus). This situation is given approximately for air-filled rock at standard room temperature and pressure (Mavko et al., 1998). The deformation behaviour is characterized by the two frame or rock skeleton moduli *k'; μ'*:

- The effective bulk modulus for the dry rock $k_{dry} = k'$
- The effective shear modulus for the dry rock $\mu_{dry} = \mu'$.

The right side describes the "fluid-saturated case." The deformation behaviour is characterized by two moduli (J.H. Schön, 2011):

1.- The effective bulk modulus for the saturated rock $k_{sat} > k_{dry} = k'$

2.- The effective shear modulus for the saturated rock, which is identical to the effective shear modulus for the dry rock $\mu_{sat} = \mu_{dry} = \mu'$, because the pore fluid does not contribute to the shear moduli.

The effective bulk modulus for the saturated rock k_{sat} results from the combined effect of the deformation of the rock skeleton, the solid components, and the fluid. The fluid contributes to the compression resistance.The derivation considers the coupled contributions to the total volume change and the participating pressure components (effective pressure and pore pressure). The resulting bulk modulus for the saturated rock is therefore greater than the dry rock (note that in the equation the deformation is thus smaller). The second term gives the "modulus magnification" as a result of the way that pore fluid is effected by and interacts with solid components. This can be expressed by the following equation (J.H. Schön, 2011)

$$k_{sat} = k_{dry} + \frac{(1-\frac{k_{dry}}{ks})^2}{\frac{\phi}{k_{fl}} + \frac{1-\phi}{k_s} - \frac{k_{dry}}{k_s^2}} \tag{18}$$

$$\frac{k_{sat}}{k_s - k_{sat}} = \frac{k_{dry}}{k_s - k_{dry}} + \frac{k_{fl}}{\phi\,(k_s - k_{fl})} \tag{19}$$

Where:

k_{sat} is the effective bulk modulus of the rock with pore fluid

k_{dry} is the effective bulk modulus of the drained or dry rock ("framework")

k_s Bulk modulus of the rock constituent

k_{fl} is the bulk modulus of the pore fluid

Ø is the porosity.

The process of a fluid substitution for a porous rock with porosity Ø in practice has the following steps (J.H. Schön, 2011):

Step 1: Gather the components' material properties:

Moduli: k_s (solid mineral component), $k_{fl,1}$ (fluid 1), $k_{fl,2}$ (fluid 2).

Densities: ρ_s (solid mineral component), ρfl,1 (fluid 1), ρfl,2 (fluid 2).

Step 2: Taken from the velocities' measurements at saturation with fluid 1 ($V_{P,1}$,$V_{S,1}$) and the porosity Ø. Then calculate the effective bulk moduli $k_{sat,1}$,$\mu_{satl,1}$ (use Equations 2 and 3).

Step 3: Calculate k_{dry} = k' (using Equation 18).

Step 4: Calculate effective bulk modulus for the replaced fluid saturation 2 (use

equation 18).

Step 5: Calculate density for fluid saturation 2 with $\rho = (1 - Ø)\,\rho_s + Ø \cdot \rho_{fl,2}$.

Step 6: Calculate the velocities for rock with fluid saturation 2 with new parameters using Equations (2) and (3).

2.2.2 Wave Velocity – P wave and S wave

P wave

Primary (P or compressional) waves travel trough all types of materials including solids, liquids and gases. In the earth, P-waves travel at speeds between 1 and 14 km/s. This, depending on the rock type, is the exact velocity (Leiv J.,2007).

The motion produced by a P-wave is an alternative compression and expansion of the material. The ground is deformed along the direction that the wave is travelling (see figure 12):

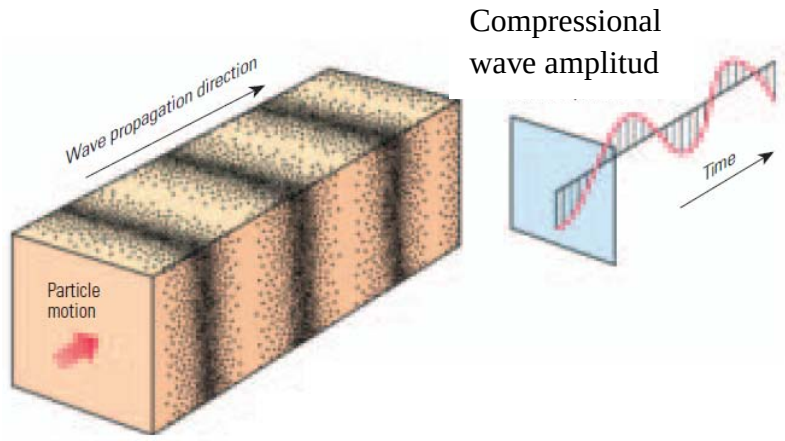

Figure 12: P-wave propagation (Jakob B.U. Haldorsen, Et al 2006).

S wave

Shear (S or secondary) waves travel through solids but not through liquids and gases. These waves travel at speeds between 1 and 8 km/s within the earth. The precise velocity depends on the rock type. S-waves vibrate the ground in a shearing motion. The movement is perpendicular to the direction that the wave is travelling (see figure 13):

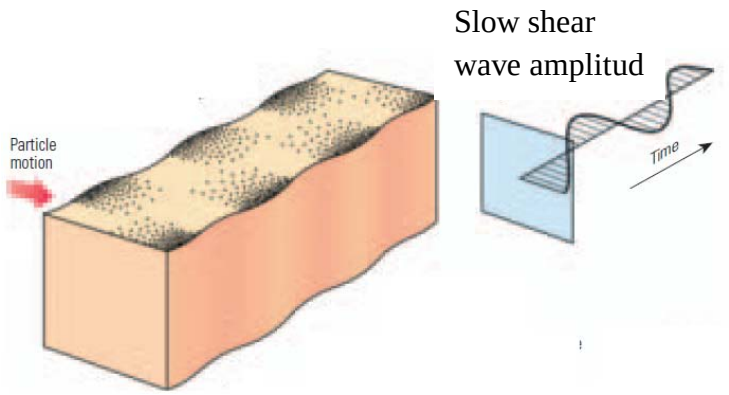

Figure 13: S-wave propagation (Jakob B.U. Haldorsen, Et al 2006)

P- and S-waves are called elastic waves because they deform the earth elastically. The rock returns to its original shape and position after the wave has passed through. An example of a non-elastic wave is a shock wave. This type of wave essentially changes the medium through which it circulates. Elastic waves are also called seismic waves. Elastic or seismic waves can be generated from a controlled source like the airgun used in seismic marine acquisition, or from various other sources (Leiv J.,2007).

3 Overview of the methodology applied

The methodology used is summarized briefly in the Diagram below:

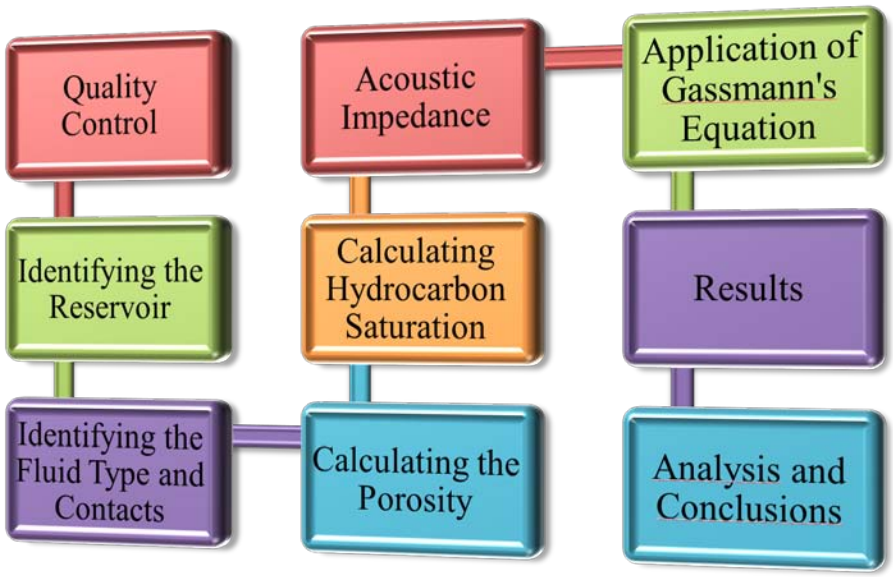

Figure 14: Diagram of the methodology applied.

3.1 Quality Control

As soon as the set data log is available it is necessary to ensure the quality of the logs as is outlined below (Darling, 2005):

1. Verify that the logger's TD and last casing shoe depths roughly match (TVD) those from the last daily drilling details, in our case the data log is in (TVD) True vertical depth.

2. Ensure that the ground level and rig floor elevation locations are correct. As far as this study is concerned the Datum is relative to the sea level.

3. Corroborate values exceeding the appropriate range. In order to correct any data out of the range it is enough to use a cut-off.

4. Check that the available log curves are on depth with each other.

5. Verify whether there are invaded zones. In this study drilling fluids were not observed invading the formation.

Having verified each one of the pervious steps, it is necessary to ensure that the arrangement scales on the log print are regular with other wells or usually conventional industry norms. These are normally from left to right, outlined as follows (Darling, 2005):

- Caliper: from 8 to 18”
- Sonic log: from 140 to 40 ms/ft
- Neutron log: 0.45 ± - 0.15 (porosity fraction)
- Density: from 1.95 to 2.95 g/cc
- Resistivity log: 0.2–2000 Ohm.m on logarithmic scale
- Gamma Ray: from 0 to 50 API

Finally, in this study “Clastic reservoir” was assumed. This was because in a few no-clastic reservoirs it was discovered that, due to the presence of radioactive minerals in sand, the Gamma Ray, is not a good indicator of sand.

3.2 Identifying the reservoir

3.2.1 Gamma Ray

In the majority of clastic reservoirs, the GR curve shows a considerable decrease when in the presence of clean sands, thus rendering it an important lithology indicator. By contrast, this behaviour will be the opposite when the presence of clays or shales is reported in the reservoir. In order to plot the Gamma Ray on the same scale of Caliper, it is necessary to perform "rescaling", which transforms Gamma ray values on a scale of 0-1, using the maximum and minimum values of the Gamma Ray log as shown below:

$$\text{GR (0-1)} = \frac{GR - GRmin}{GRmax - GRmin} = \frac{51.685 - 0}{100 - 0} = 0.51 \qquad (20)$$

Where:

GR = measured value.

GRmax = maximum value on the GR scale.

GRmin = minimum value on the GR scale.

Having calculated the value GR (0-1), it is then transferred to the Caliper scale, which ranges between 8 -18". Using the Caliper scale, you need to subtract the maximum Caliper Value from the minimum Caliper value. Then, it is necessary to add the minimum value of the Caliper as is shown below:

$$GR_{rescaling} = GR\ (0\text{-}1) * (HCAL_{max} - HCAL_{min}) + HCAL_{\text{initial value}} \quad (21)$$

$$GR_{rescaling} = 0.51 * (18 - 8) + 8 = 13.1$$

13.1 will be the new Gamma Ray value in the Caliper scale.

3.2.2 Neutron with Density logs (reservoir hydrocarbon potential)

With the aim of determining the hydrocarbon reservoir, one of the most important indicators of reservoir rock is from the behaviour of the neutron/density logs, with the density going in the left direction (low density) and crossing the neutron curve. The larger the crossover between the neutron and density logs, the better the quality of the hydrocarbon reservoir. Nevertheless, gas zones will show a larger intersection for specified porosity than water or oil zones.

3.2.3 Shale volume (Vsh)

The Shale volume is a visual representation of the GR curve in a scale between 0 and 1. It is used in order to identify more easily the present lithology in the reservoir. Therefore, according to the reservoir quality, this acts as a lithology discriminator. The shale volume is defined as:

$$Vsh = \frac{GR - GRsa}{GRsh - GRsa} \quad (22)$$

Where: GR measurement value from the Gammay Ray log. GRsa represents the clean sand's value from the Gammay Ray log. GRsh represents the shale value from Gammay Ray log. According to Darling 2005, for GRsh, it is recommended not to take the highest observed value. The values taken in this survey correspond to:

Grsa (clean sands) =20

GRsh (shale) = 90

3.3 Identifying the fluid type and contacts (owc, gwc, goc)

3.3.1 Resistivity ohm

At the beginning, it is necessary to contrast the deepest resistivity with the density log to look for any sign of oil, gas, or water. Usually, the resistivity and density will show a "Mirror Image or Mae West" in hydrocarbon sands, whereas with water sand, the curves will present the same pattern, going in the same direction from left to right, also known as "Tramline". Nevertheless, some zones will not show this kind of behaviour, the reasons for which, will be show below (Darling 2005):

- When there are invasion evidences the hydrocarbon response can be totally masked. However in this study invasion proofs were not reported.
- As it is known, with the existence of finely laminated sand between shales, the recorded resistivity can remain low.
- In the case where the water salinity is especially elevated, the resistivity decreases in clean sands.

3.3.2 Neutron and Density logs

In order to plot the Neutron and Density logs on the same scale, it is necessary to perform the analogous process performed in the Gamma Ray and Caliper plot (see section 3.2.1). As it is known, the gas zones will show a larger neutron/density intersect than oil or water zones. Therefore, in the presence of clean sands it possible to identify the Gas-Oil Contact quite straightforwardly. Nevertheless, according Darling 2005, the GOCs will be recognized rightly in just under 50% of most cases. In addition, it is recommended to combine it with other techniques and compare them with each other.

3.3.3 Formation-pressure plots (gradients)

Pressure data is certainly appreciated by petro-physicists in determining the fluids which are present in the formation process. Therefore, in order to identify the formation fluids it is possible to use the correlation between pressure and depth, as shown below:

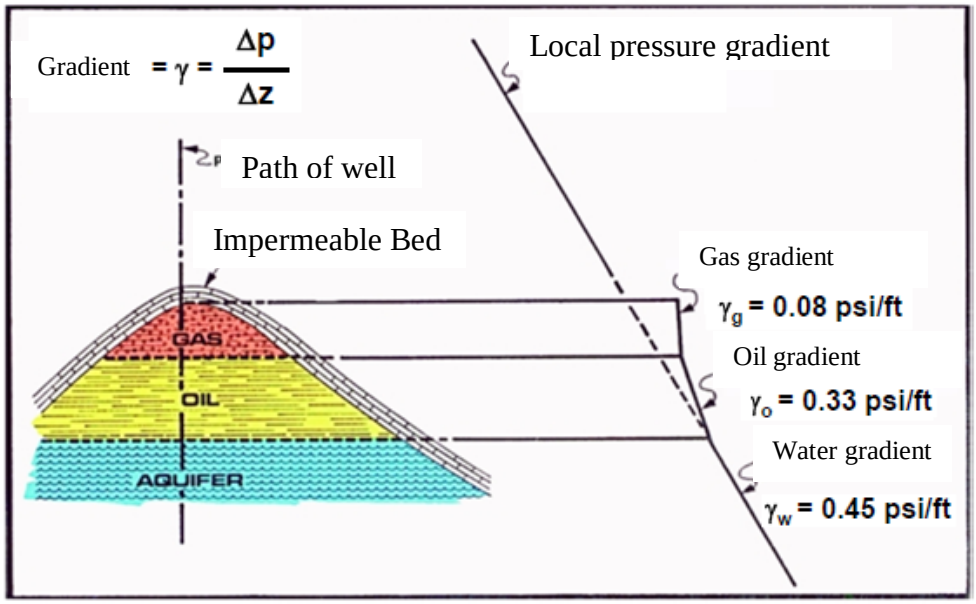

Figure 15: Fluid model gradient in hydrocarbon reservoir.

γg = 0.08 psi/ft, = 1.8 kPa/m = 0.02 $Kg_f/cm^2/m$

γo = 0.34 psi/ft, = 7.5 kPa/m = 0.07 $kg_f/cm^2/m$

γw = 0.45 psi/ft = 10.2 kPa/m = 0.10 $kg_f/cm^2/m$

3.4 Calculating the porosity

Porosity should be calculated from the density log by using the following equation:

$$\emptyset = \frac{\mathrm{rho_m} - \mathrm{Density}}{\mathrm{rho_m} - \mathrm{rho_f}} \tag{23}$$

Where:

rho_m = matrix density (in g/cc) and *rhof* = fluid density (in g/cc).

For sand, rho_m is between 2.64 and 2.67 g/cc. Fluid density, rho_f, depends on the formation fluid properties and mud type. In this survey the values which have been taken are outlined below:

Matrix density (g/cc) = 2.66

Fluid density in water (g/cc) = 1

Fluid density in oil (g/cc) = 0.9

According to Darling 2005, the porosity which has been calculated by the density log will be the total porosity. Therefore, water bound clays is also taken into consideration.

Having calculated the total porosity, it is vital to verify any area where washouts have resulted in incorrect large density measurements. As a result, a large porosity value is exhibited. Also in some cases it is enough to use a cut-off.

3.5 Calculating hydrocarbon saturation - Archie's equation

In this study, Archie's equation was used in order to calculate the water saturation:

$$S_w = [(R_t/R_w)*\emptyset^m]^{(-1/n)} \quad (24)$$

Where:

R_w = formation water resistivity (ohm.m)

m = the cementation, or porosity, exponent.

S_w = water saturation.

n = saturation exponent.

According to Darling 2005, the reasons why you should never use the density or neutron log for calculating porosity in sandstones are explained below:

- The neutron can be deeply affected by the quantity of chlorite in the reservoir. This occurs in clay minerals or formation water.
- Gas will alter the neutron log in an irregular way.

In order to calculate de hydrocarbon saturation, it can be obtained easily by the follow equation:

$$S_{hyc} = 1 - Sw \quad (25)$$

3.6 Overview of Acoustic Impedance

As it is known, the Acoustic Impedance (AI) is defined as the interference of the sound waves through a medium, and it is given by the equation:

$$AI = \rho * V_p \tag{26}$$

Where ρ = in situ density and V_p= P wave velocity, the unit is expressed in $kg/m^2/s$.

Consequently, an AI may be calculated from the density and sonic logs. However, before calculating the AI, it is essential to do an accurate quality control for invasion or washouts. Additionally, the logs must be correct for Datum or well deviation.

3.7 Application of Gassmann's Equation

Gassmann's equations link the bulk modulus of a rock to its fluid properties, frame, pore, and (see also section 2.3.1). The saturated bulk modulus of a rock is shown by Gassmann's theory (Gassmann, 1951) (outlined below):

$$k_{sat} = k_{frame} + \frac{(1-\frac{k_{frame}}{kmatrix})^2}{\frac{\phi}{k_{fl}} + \frac{1-\phi}{k_{matrix}} - \frac{k_{frame}}{k^2_{matrix}}} \tag{27}$$

Where:

Ø Porosity (fraction)

k_{matrix} Bulk modulus of Rock Matrix (GPa, where GPa = 10^9Pa)

k_{frame} Dry-frame Bulk modulus (GPa)

k_{sat} Bulk modulus of Saturated rock (GPa)

K_{ft} Bulk modulus of pore fluid (GPa)

As is well known, shear modulus is autonomous of the pore fluid and supposed constant through the fluid replacement. By using Wireline log data's mean average, it is possible to calculate the Shear modulus (μ) and Bulk modulus (K_{sat}), from density and seismic velocities (Kumar, 2006):

$$k_{sat} = r\,(V^2_p - 4/3 \cdot V_S^2) \tag{28}$$

And

$$\mu = \rho \cdot V_S^2 \tag{29}$$

Where:

μ Shear modulus (GPa)

ρ Densities from Data logs (g/cm^3, where g/cm^3 = 1000 kg/m^3)

r Bulk density of the rock (g/cm^3)

V_S velocities of S waves (km/s, where km/s = 1000 m/s)

V_P velocities of P waves (km/s)

In order to use Gassmann's equation (18 or 27), it is necessary to elicit the bulk modulus from the porous rock frame (Dry-frame Bulk modulus), $K_{frame,}$ Subsequently we can calculate the bulk modulus of rock saturated by another fluid, such as: Oil, Brine or Gas.

Dry-frame Bulk modulus, K_{frame}, corresponds to the property of a rock with several quantities of moisture present. Hence, the appropriate way to utilize K_{frame} is by the porous rock frame modulus. However, it is necessary to identify the shear and bulk moduli, in addition to the pore's shear and bulk moduli with other fluids (Nawras, 2013).

3.1.1 Rock Properties:

The correlation in equation (28) links the bulk modulus to the bulk density, shear velocity, and compressional velocity.

The shear modulus (μ) is characterized as the relation of shear stress to shear strain (equation 29).

Likewise, Vs and ρ_B can be determined by lab work or log analysis. However, the shear modulus is not susceptible to fluid filling the pores, and so: $\mu_{sat} = \mu$ (Biot, 1956).

The bulk modulus is susceptible to pore-fluid formation, whereas the shear modulus is not. As a result, the shear modulus cannot be modified by fluid replacement. This theory is one of the most essential concepts regarding the application of Gassmann's equation.

In order to calculate the bulk density, ρ_B, the correlation below connects matrix density (ρ_{matrix}), fluid density (ρ_{ft}) , the porosity (Ø), and permits, to calculate: ρ_b (Equation 30):

$$\rho_b = \rho_{matrix}(1 - Ø) + \rho_{ft} \cdot Ø \tag{30}$$

On the other hand, the porosity can be calculated either from the core-analysis or from wireline logs.

3.1.2 Matrix properties:

In order to estimate the bulk modulus of the matrix, it is necessary to identify the mineral arrangement of rock, which is derived from laboratory tests on cores. If we do not know this core data, the lithology could be taken to be an arrangement of clay and raw quartz materials. The clay proportion can be obtained from the volume shale curve (V_{sh}), from the wireline log data (specifically Gamma-ray log). However the representative shale comprises more or less 30% of the other materials (generally quartz) and 70% of clay. When the mineral proportions are obtained, K_{matrix} is calculated by Voigt-Reuss-Hill (VRH) averaging method (Hill, 1952). Inputs used for K_{matrix} computation are $K_{clay,}$ V_{sh}, and K_{qtz}. The K_{matrix} is obtained as follows:

$$K_o = K_{vrh} = \frac{1}{2}\left([V_{clay}K_{clay} + V_{qtz}K_{qtz}] + \left(\frac{V_{clay}}{K_{clay}} + \frac{V_{qtz}}{K_{qtz}}\right)^{-1}\right) \tag{31}$$

Where V_{clay} and V_{qtz} are:

$$V_{clay} = 70\% \cdot Vs_h \quad (32)$$

and

$$V_{qtz} = 1 - V_{clay} \quad (33)$$

Subsequently, the density ρ_{matrix} is calculated through of mean of densities of each different mineral as shown below:

$$\rho_{matrix} = V_{clay} \cdot \rho_{clay} + V_{qtz} \cdot \rho_{qtz} \quad (34)$$

Where the following data can be assumed:

ρ_{clay} Clay density = (2.58 g/cm^3)

ρ_{qtz} Quartz density = (2.65 g/cm^3)

K_{clay} = (20.9 GPa)

K_{quartz} (36.6 GPa),

Text books confirm these values (as Mavko, 1998). Likewise, these are constant values which are seen throughout Gassmann's fluid replacement theory (Kumar, 2006).

3.1.3 Fluid properties:

Pore fluid density and Bulk modulus are obtained by averaging the singular fluid proportion. Therefore, it is possible to obtain properties of every type of fluid such as: oil and brine.

3.1.3.1) Density and Bulk Modulus of Brine

As exhibited below, the Bulk modulus of Brine is calculated through its density and P wave velocity:

$$K_{brine} = \rho_{brine} \cdot V^2_{brine} \times 10^{-6} \quad (35)$$

Where:

V_{brine} = P-wave velocity through brine (m/s)

K_{brine} Brine bulk modulus (GPa)

ρ_{brine} Brine density (g/cm^3)

The proportion of brine is estimated by pure water with high salt solution. According to Batze and Wang (1992), it is possible to calculate this by using the following equation:

$$\rho_{brine} = \rho_w + 0.668S + 0.44S^2 + 10^{-6} S[300P - 2400PS + T(80 + 3T - 3300S - 13P + 47PS)] \quad (36.a)$$

Where:

P in-situ Pressure (MPa)

T in-situ Temperature (ºC)

S Salinity (as weight fraction)

ρ_w The water density (g/cm^3) is shown below:

$$\rho w = 1+10^{-6}(-80T-3.3T^2+0.00175T^3+489P-2TP+0.016T^2P-1.3x10^{-5}T^3P-0.333P^2-0.002T\cdot P^2) \quad (36.b)$$

V_{brine} (m/s) P The brine's wave velocity is shown below:

$$V_{brine}=Vw+S(1170-9.6T+0.0055T^2-8.5x10^{-5}T^3+2.6P-0.0029TP-0.0476P^2)+S^{1.5}(780-10P+0.16P^2)-1820S^2 \quad (37)$$

Where V_w (m/s) is P-wave velocity in pure water. This is approximated by:

$$V_w = \sum_{i=1}^{5}\sum_{j=1}^{4} w_{ij} T^{i-1} P^{j-1} \quad (38)$$

Where constants are W_{ij} (see Appendix B).

Density and Bulk Modulus of Gas

As is well known, in a reservoir, gas density and bulk modulus depend on the temperature, gas composition and pressure. Natural gas is a mixture of several gases, which are differentiated by specific gravity G in API. This shows us the relation between the gas density and the air density, which when over atmospheric pressure is at 15.6ºC. According to Batzle and Wang (1992), density of gas can be represented in the following equation:

$$\rho_{gas} \cong \frac{28.8\,GP}{ZR\,(T+273.15)} \tag{39}$$

Where R is the gas constant and Z is the compressibility factor can be calculated as follows:

$$Z = \left[0.03 + 0.00527\left(3.5 - T_{pr}\right)^3\right] P_{pr} + \left(0.642T_{pr} - 0.007T_{pr}^4 - 0.52\right) + E \tag{40}$$

and

$$E = 0.109(3.85 - T_{pr})^2 e^{-[-(0.45+8(0.56-1/T_{pr})^2]P_{pr}^{1.2}/T_{pr}} \tag{41}$$

In this last equation, pseudo-reduced pressure P_{pr} and pseudo-reduced temperature T_{pr} can be calculated as follows:

$$T_{pr} = \frac{T+237.15}{94.72+170.75G} \tag{42}$$

$$P_{pr} = \frac{P}{4.892-0.4048G} \tag{43}$$

Alternatively, K_{gas} (GPa), is calculated like this (Batzle, 1992):

$$K_{gas} \cong \frac{P}{(1-\frac{Ppr}{Z}\frac{\partial Z}{\partial P_{pr}})_t}\ \frac{\Upsilon_0}{1000} \tag{44}$$

Where:

$$\Upsilon_0 = 0.85 + \frac{5.6}{P_{pr}+2} + \frac{27.1}{(P_{pr}+3.5)^2} - 8.7\, e^{-0.65(P_{pr}+1)} \quad (45)$$

$$\left(\frac{\partial Z}{\partial P_{pr}}\right)_t = 0.03 + 0.00527\,(3.5 - T_{pr})^3 + 0.109(3.85 - T_{pr})^2 F \quad (46)$$

$$F = -1.2\frac{P_{pr}^{0.2}}{T_{pr}}\left[0.45 + 8\left(0.56 - {}^{1}/_{T_{pr}}\right)^2\right] e^{-\left[0.45+8\left(0.56-{}^{1}/_{T_{pr}}\right)^2\right]P_{pr}^{1.2}/T_{pr}} \quad (47)$$

3.1.3.3) Density and Bulk Modulus of Oil

Oil encompasses a quantity of gas which is represented by the GOR (gas to oil ratio) value. As well as gas, bulk modulus and oil density depend on pressure, oil composition, and GOR and temperature. P wave velocity and oil density are outlined below (Batzle 1992):

$$\rho_{oil} = \frac{\rho_s + \left(0.00277P - 1.71x10^{-7}P^3\right)(\rho_s - 1.15)^2 + 3.49x10^{-4}P}{0.972 + 3.81x10^{-4}(T+17.78)^{1.175}} \quad (48)$$

And

$$V_{oil} = 2096\sqrt{\frac{\rho_{ps}}{2.6-\rho_{ps}}} - 3.7T + 4.64P + 0.0115\left(\sqrt{\frac{18.33}{\rho_{ps}} - 16.97} - 1\right)TP \quad (49)$$

Where P wave velocity through the oil is V_{oil} (m/s), and the oil density is ρ_{oil} (g/cm^3). In addition, the saturation density is ρ_s and the pseudo density is ρ_{ps}, all of which are shown below:

$$\rho_s = \frac{\rho_o + 0.0012R_G G}{B_o} \quad (50)$$

$$\rho_{ps} = \frac{\rho_o}{(1+0.001R_G)B_o} \quad (51)$$

The Gas to oil ratio is R_G (l/l). The oil density ρ_0 (g/cm^3) is the hypothetical oil density, (calculated at 15.6ºC). With regards to atmospheric pressure, (known as the formation volume factor) please see the following equation:

$$B_0 = 0.972 + 0.00038\,(2.495\,R_G\sqrt{G/\rho_0} + T + 17.8)^{1.175} \quad (52)$$

Following on from this equation we now know the density and P wave velocity of the oil. Therefore, it is possible to obtain k_{oil} by:

$$K_{oil} = \rho_{oil} V_{oil}^2 x 10^{-6} \quad (53)$$

As is well known, fluid in reservoir pore spaces is due to hydrocarbon and brine proportion. Density and Bulk modulus can be obtained by inverting the bulk modulus' mean. This theory is also known as "Wood's equation", (Kumar, 2006).

$$\frac{1}{K_{fl}} = \frac{WS}{K_{brine}} + \frac{HS}{K_{hyc}} \quad (54)$$

$$\rho_{fl} = WS\rho_{brine} + HS\rho_{hyc} \quad (55)$$

Where:

K_{hyc} = Hydrocarbon Bulk modulus

ρ_{hyc} . = Hydrocarbon Density

HS = Hydrocarbon Saturation

WS = Water saturation

When the hydrocarbon is oil, it makes the following change:

$$K_{hyc} = K_{oil} \quad (56)$$

And

$$\rho_{hyc} = \rho_{oil} \quad (57)$$

For gas it is necessary to perform the following change:

$$K_{hyc} = K_{gas} \quad (58)$$

and

$$\rho_{hyc} = \rho_{gas} \quad (59)$$

3.1.4 Frame Property:

With regards to calculating the Frame Bulk Modulus, this data can be estimated by the use of experimental relationships, laboratory tests and data logging. When data is obtained from wireline tests, K_{frame} is estimated by Gassmann's equation (Equation 27) (Zhu and McMechan, 1990):

$$K_{frame} = \frac{K_{sat}\left(\frac{\phi K_{matrix}}{K_{fl}} + 1 - \phi\right) - K_{matrix}}{\frac{\phi K_{matrix}}{K_{fl}} + \frac{K_{sat}}{K_{matrix}} - 1 - \phi} \quad (60)$$

All of the parameters in equation (51) have been taken from the following prior equations: K_{matrix} (equation 31), K_{sat} (equation 28), and K_{fl} (equation 54). When fluid replacement takes place, the K_{frame} value is invariable (Kumar, 2006).

3.1.5 Algorithm

Finally, it is given an algorithm using the previous equations for a point located in a hydrocarbon reservoir (Kumar, 2006).

1) Calculate ρ_{matrix} and K_{matrix} (equation 31) (equation 34).

2) Calculate K_{brine} (equation 35) and ρ_{brine} (equation 36.a).

3) Calculate K_{hyc} (equation 56 or 58) and ρ_{hyc} (equation 57 or 59) according to the original hydrocarbon.

4) Estimate density of initial fluid ρ_{fl} (equation 55) and bulk modulus K_{fl} (equation 54) (according to steps 2 and 3). The type of hydrocarbon is characterized by initial fluid and initial water saturation.

5) Then, calculate as shear modulus (μ) (equation 29) as initial saturated bulk modulus K_{sat} (equation 28) and to obtain K_{frame} (equation 60).

6) Calculate density ρ_{hyc} (equation 57 or 59) and K_{hyc} (equation 58 or 56) of the required hydrocarbon.

7) Calculate, K_{fl} (equation 54) and ρ_{fl} (equation 55) of required fluid (from steps 2 and 7). Required fluid is characterized according to the kind of final hydrocarbon and water saturation, obtain ρ_{sat} (g/cm^3) following fluid replacement by Ø.

$$\rho_{sat} = Ø \cdot \rho_{fl} + (1 - Ø)\, \rho_{matrix} \tag{61}$$

8) Next, it is necessary to obtain the bulk modulus by using equation 27, once the fluid replacement takes place (from step 7).

9) Calculate P and S wave velocities (km/s) (equation 2 and 3) subsequent to fluid replacement by means of shear modulus from step 5, bulk modulus from step 8 and density from step 7 (Kumar, 2006).

4 Results

4.1 Main Results of Borehole Data Survey (phase 1)

Figure 16 shows the Gamma ray and Caliper logs, which are useful for lithological identification, whereas the density and porosity logs are important for identifying the types of fluid present. These logs must be compared to the resistivity and sonic logs, as is shown below:

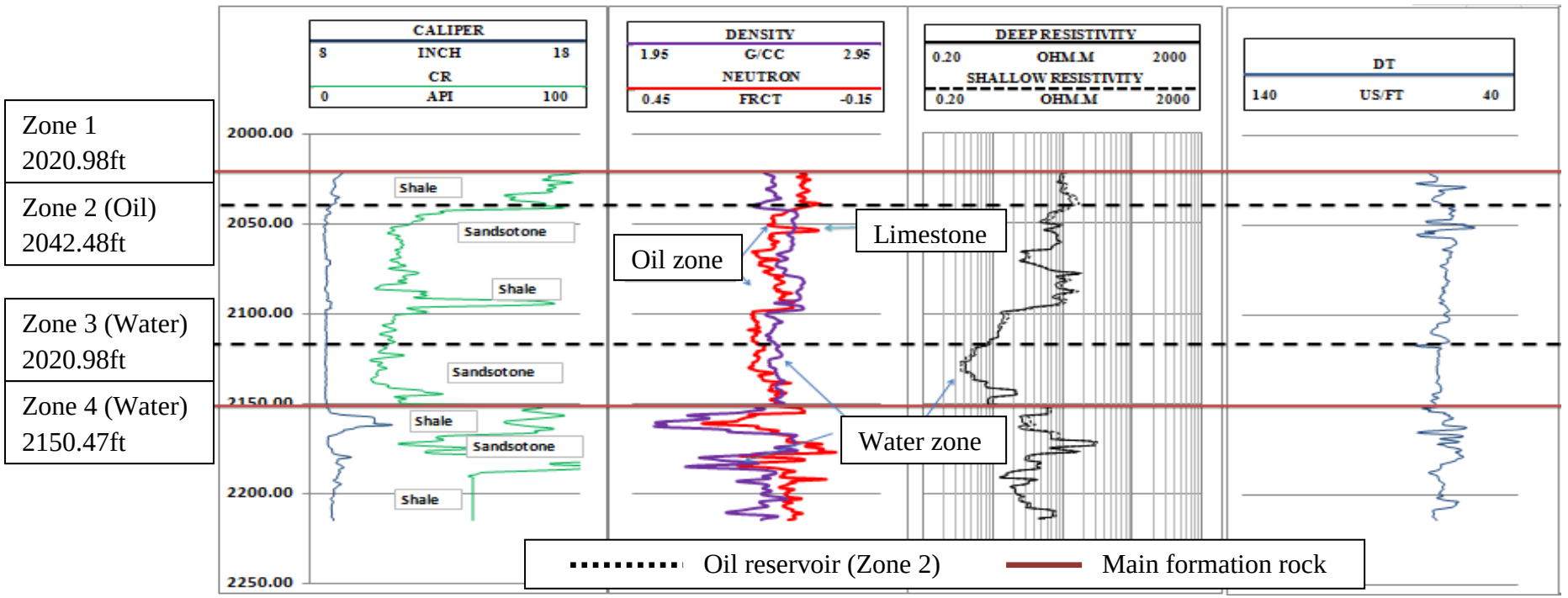

Figure 16: Report of Caliper, Gamma Ray, Density, Neutron and Sonic logs. (Reservoir and fluid identification)

Figure 17 exhibits the relationship between the shale volume and the acoustic impedances calculation, which is useful for identifying lithological interfaces. Furthermore, the water saturation and porosity estimates are shown as being crucial factors in the identification of the oil reservoir and quantification of the amount of hydrocarbon present in the porous media.

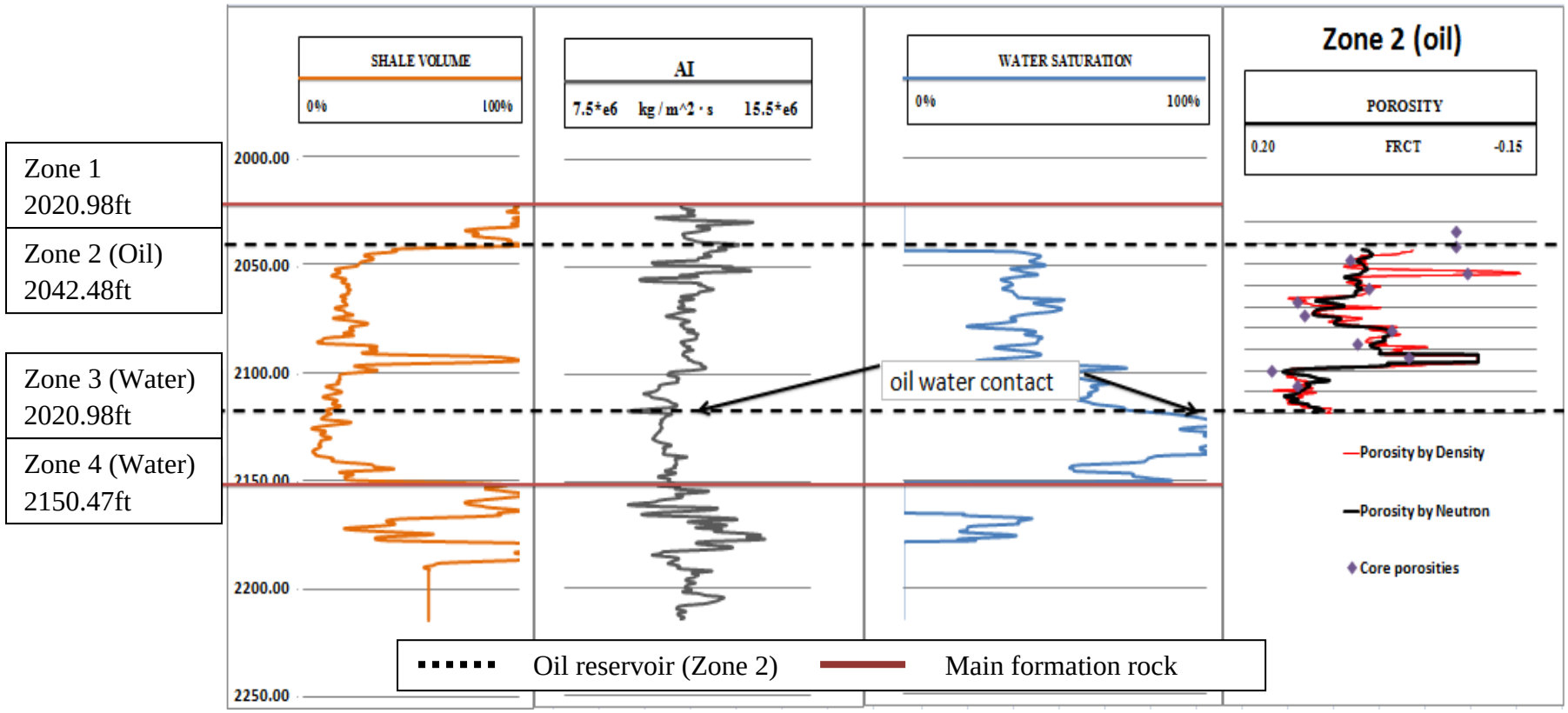

Figure 17: Report of Shale Volume, Acoustic Impedance, Water saturation and Porosity Estimation.

Table 5: Formation pressure data, between 2047.21ft – 2171.88 ft. zone 2 y 3.

Formation Pressure Data		
Depth ft (TVD)	Depth M (TVD)	Fpress (psia)
2047.21	624	5177
2066.90	630	5184.3
2086.58	636	5191.4
2106.27	642	5198.6
2119.39	646	5203.6
2129.23	649	5208.1
2140.72	652.5	5213
2171.88	662	Tight

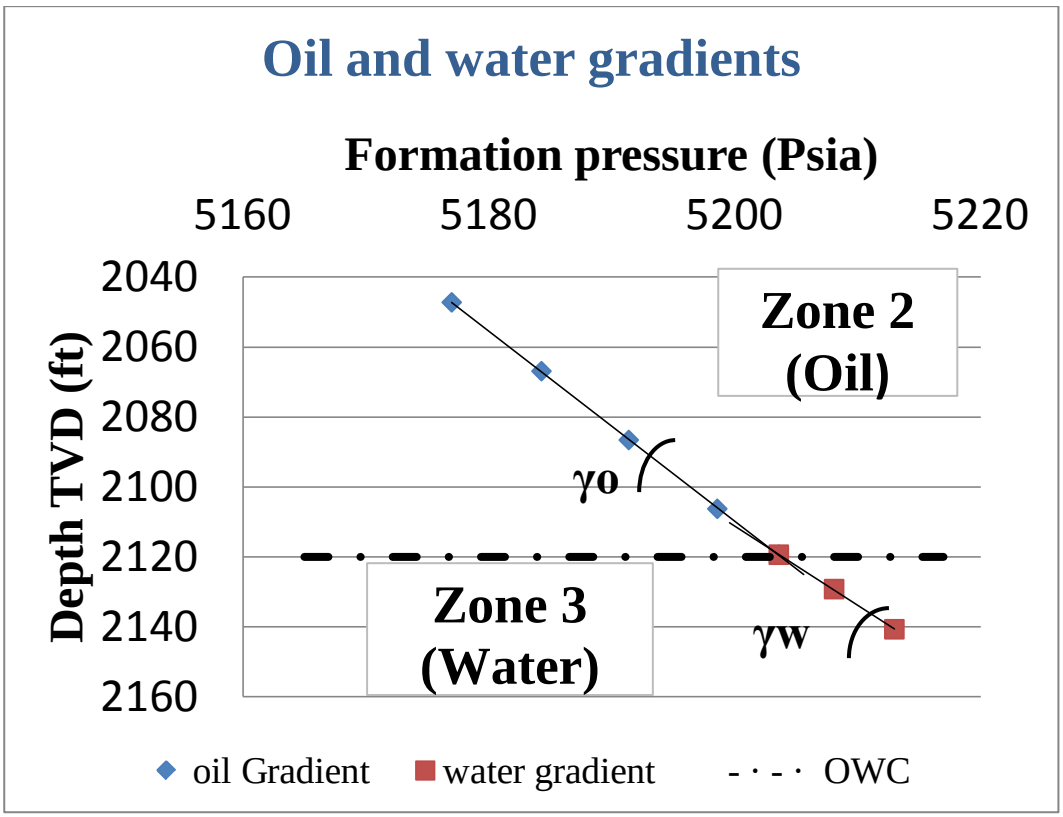

Figure 18: Formation pressure plot of zone 2 and 3, exhibiting the interception point between Oil and Water gradient.

Table 6: Identification of Oil and Water gradients present in the reservoir.

	Psia/ft
Oil Gradient (γo)	0.36
Water Gradient (γw)	0.44

Table 7: Core porosity data, between 2034.09ft – 2106.27 ft, zone 2 y 3.

Core porosities	
depth (FT)	porosity
2034.09	0.02
2040.65	0.02
2047.21	0.1105
2053.78	0.01
2060.34	0.095
2066.90	0.156
2073.46	0.15
2080.02	0.075
2086.58	0.105
2093.15	0.06
2099.71	0.179
2106.27	0.156

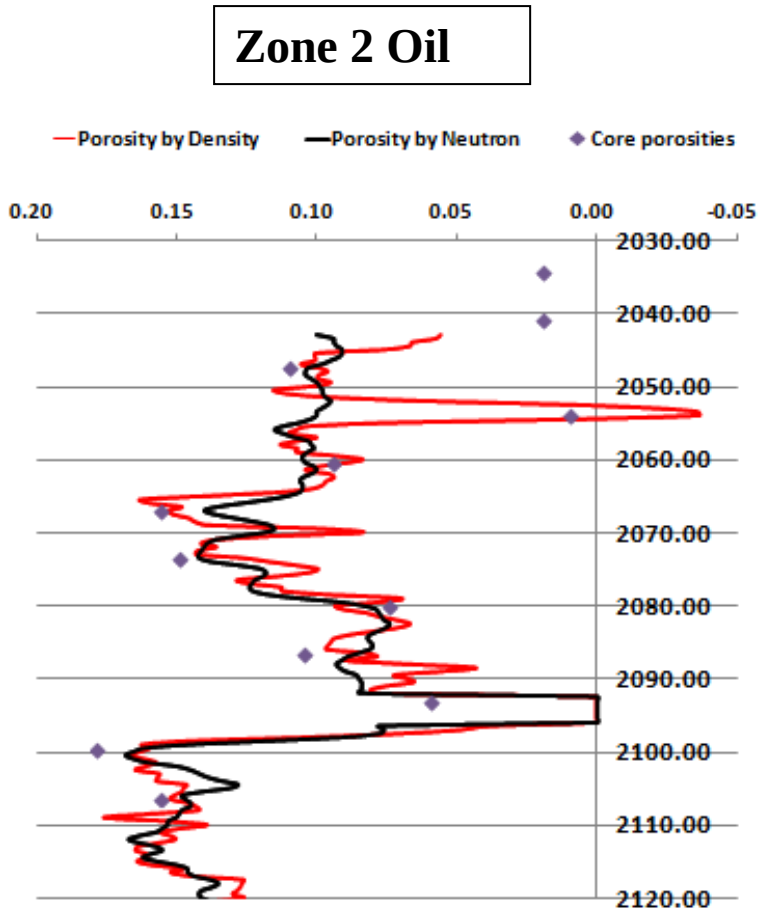

Figure 19: Calibrating the Density and Neutron logs against the Core porosity in zone 2.

Table 8: Most relevant results and averages data of the reservoir.

Zone	Top(ft)	Base(ft)	Gross(ft)	Net(ft)	Porosity Average	Sw Average
Zone 1	2020.98	2042.48	21.5	0	0	0
Zone 2 Oil	2042.48	2120.47	77.99	70.50	0.12	0.48
Zone 3 Water	2120.47	2150.47	30	30	0.13	0.89
Zone 4 Water	2150.47	2214.47	64	0	0	0

Table 9: Reporting of the lithology and thicknesses in the reservoir.

Lithology	Top(ft)	Base(ft)	Gross(ft)
Shale	2020.97	2042.29	21.32
Sandstone	2042.29	2050.50	8.20
Limestone	2050.50	2055.42	4.92
Sandstone	2055.42	2091.51	36.08
Shale	2091.51	2096.43	4.92
Sandstone	2096.43	2139.08	42.65
Silty sandstone	2139.08	2150.56	11.48
Shale	2150.56	2165.32	14.76
Sandstone	2165.32	2171.88	6.56
Limestone	2171.88	2178.45	6.56
Shale	2178.45	2214.54	36.08

Table 10: Lithological average in the reservoir.

Lithology	%
Shale	39.83
Sandstone	54.23
Limestone	5.93

4.2 Main results of Gassmann fluid substitution in zone 2 (Phase 2).

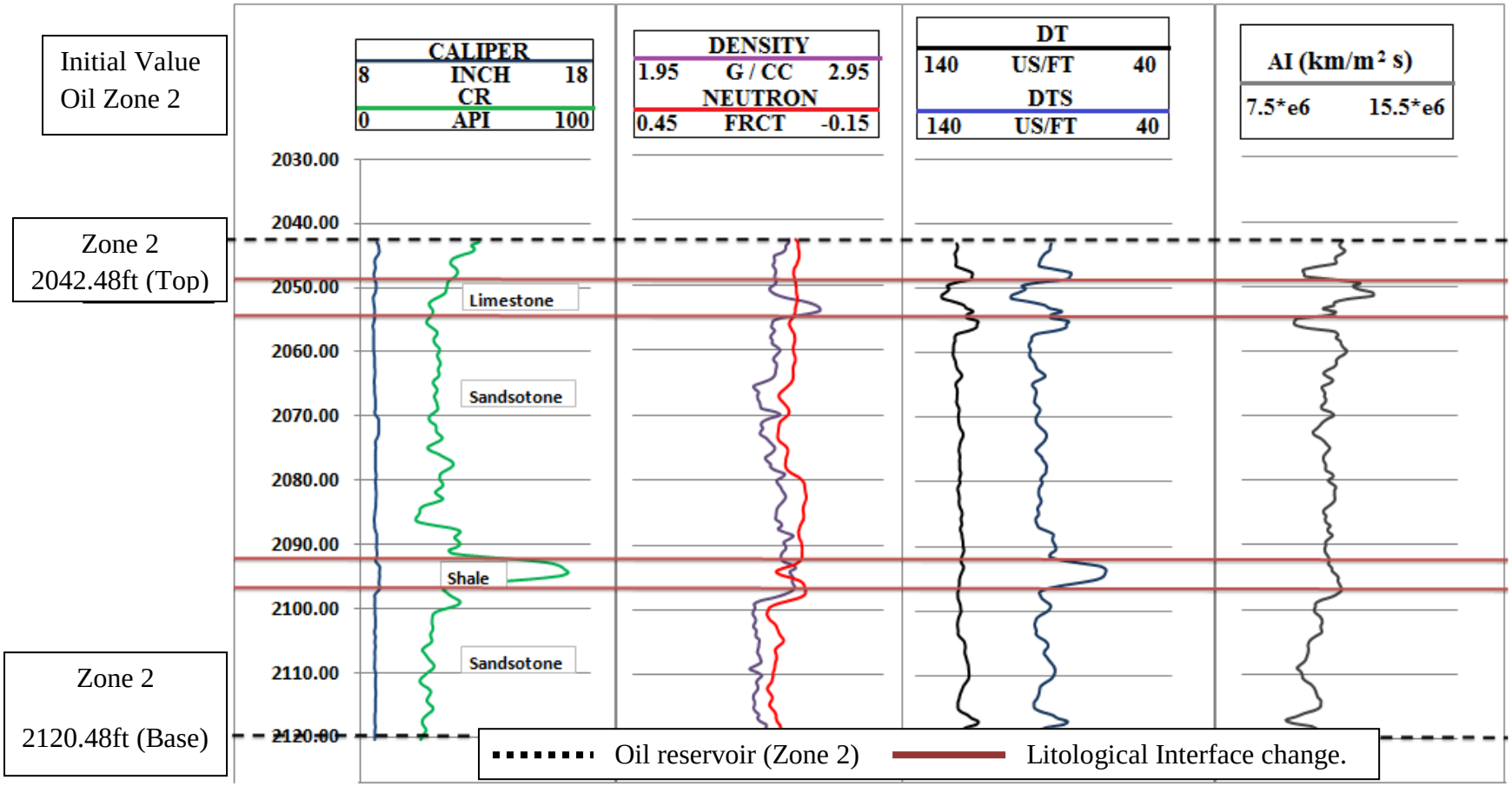

Figure 20: Zone 2, Original values before the fluid replacement modelling.

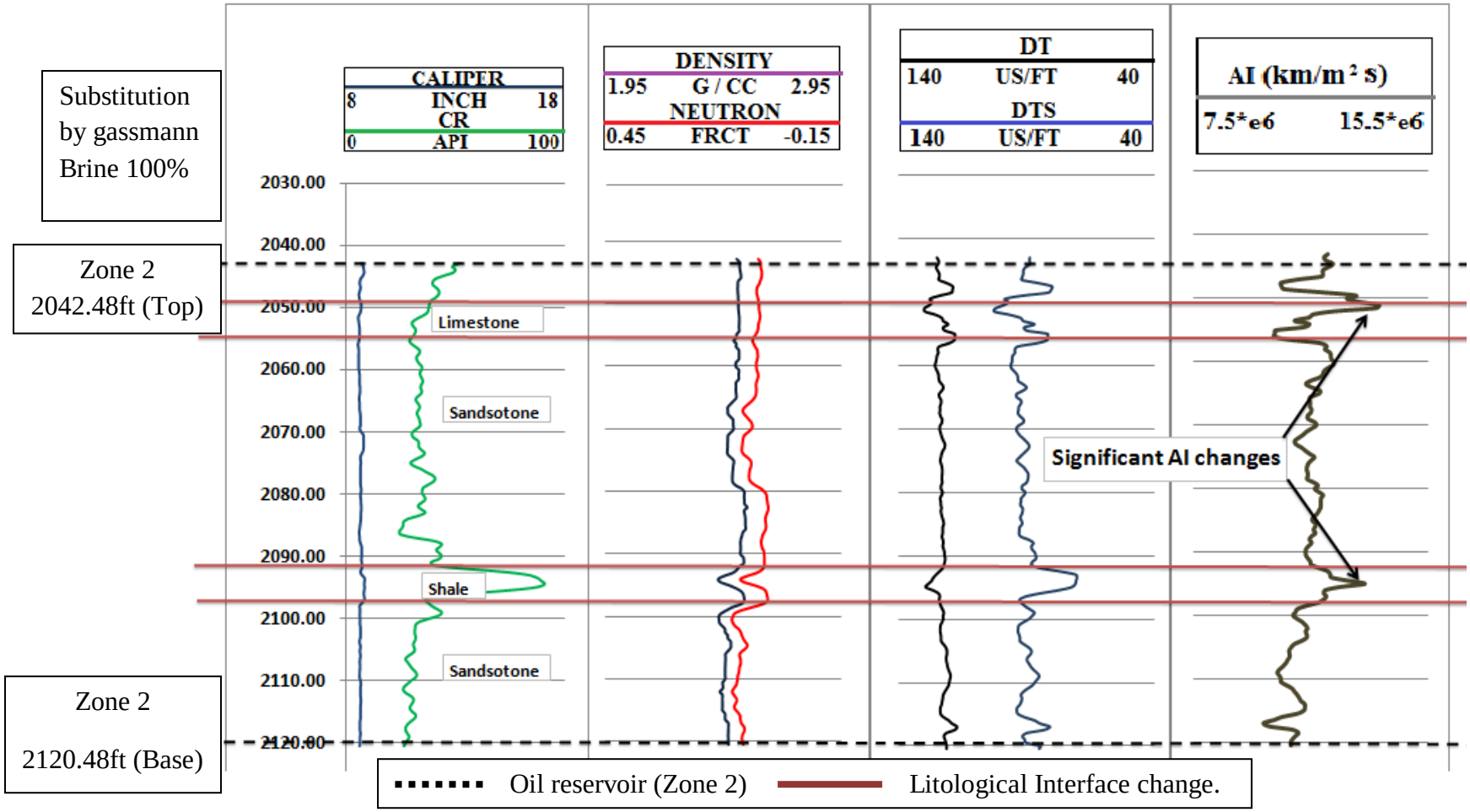

Figure 21: Zone 2 after fluid substitution, from Oil to Brine using Gassmann's equation.

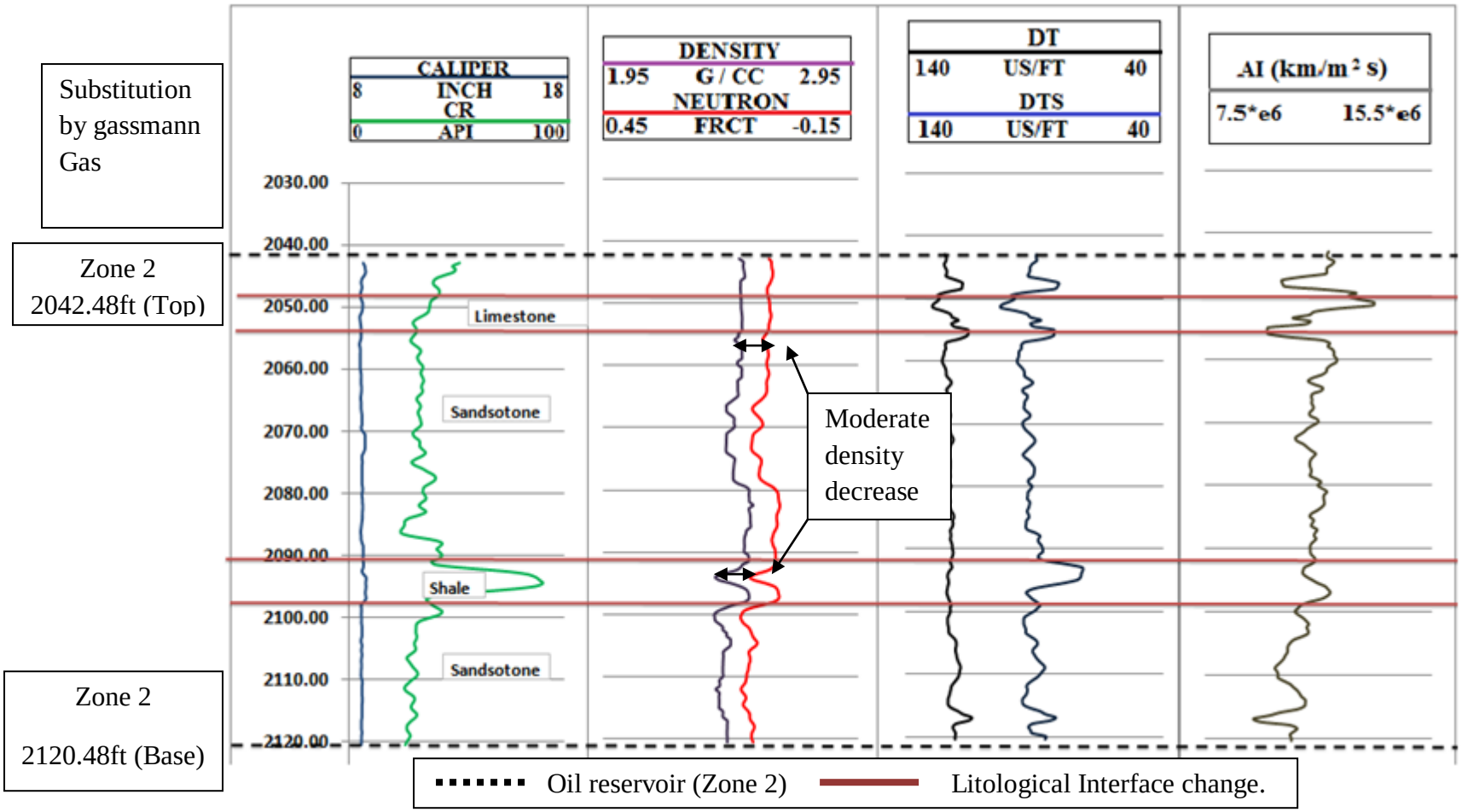

Figure 22: Zone 2 after fluid substitution, from Oil to Gas, using Gassmann's equation.

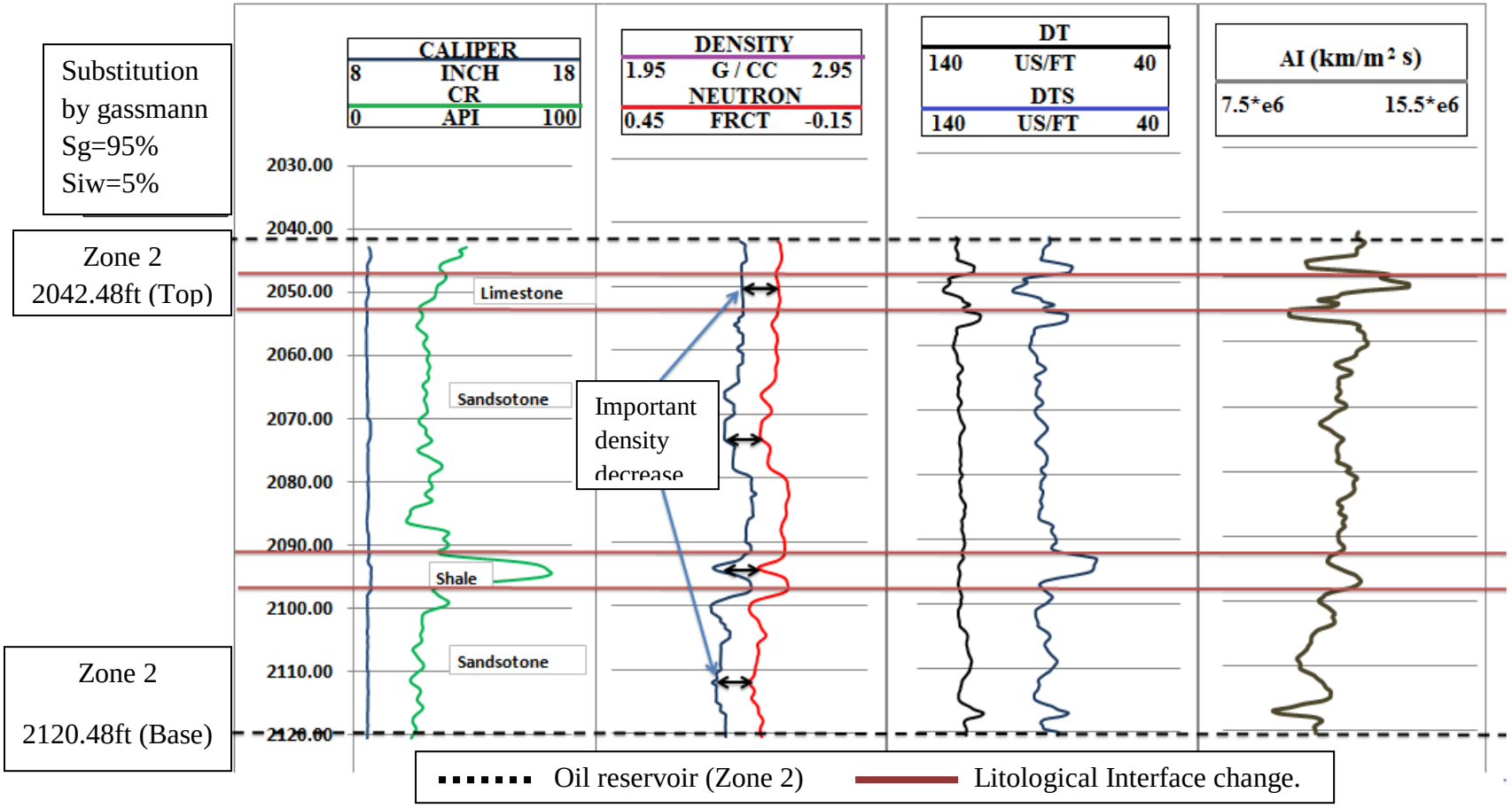

Figure 23: Zone 2 after fluid substitution, from Oil to 95% Gas and 5% Siw, using Gassmann's equation.

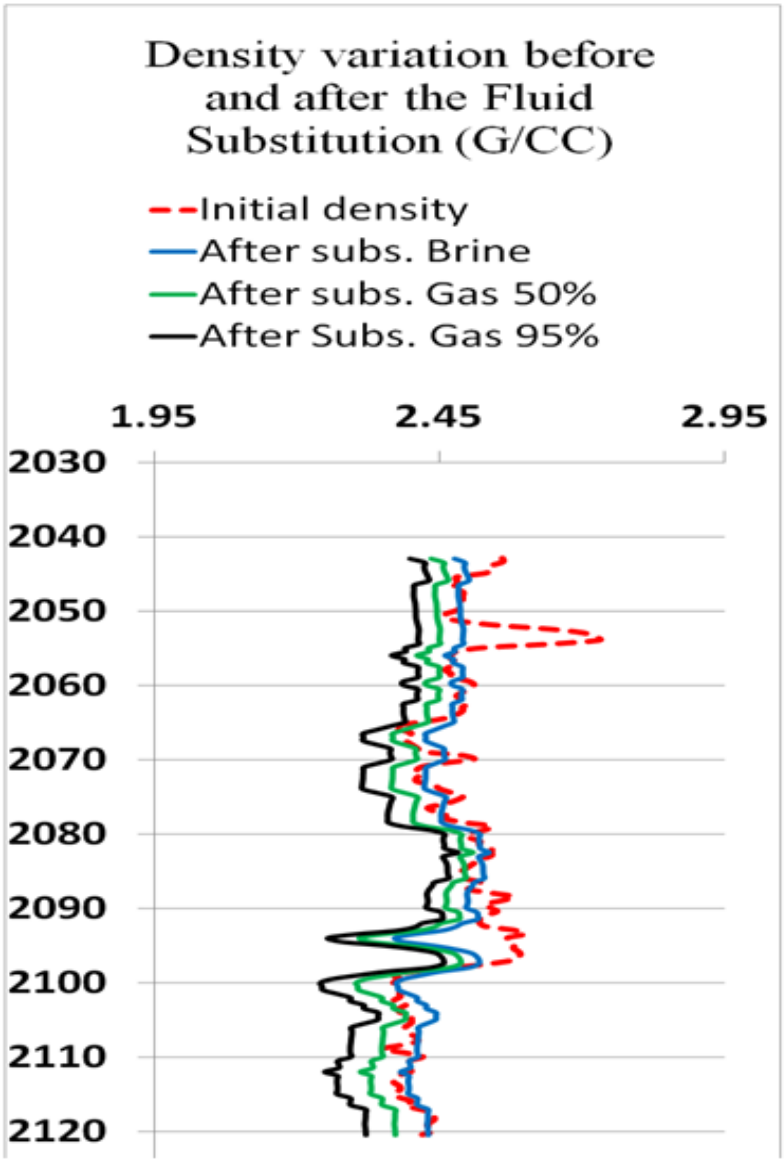

Figure 24: Density variation before and after fluid substitution modelling in Zone 2.

Table 11: Most relevant average data after Gassmann Fluid Substitution in Zone 2.

	Brine	Gas	Gas 95% and 5% brine
Density increase average %	0.44	--	--
Density decrease average %	--	2.39	4.14
AI decrease average %	--	1.57	2.47
AI increase average %	1.05	--	--

5 Analysis and Discussion of Results

Before proceeding with the data interpretation, it is necessary to check in detail if quality control was successfully performed, in order to avoid incorrect interpretations. In this study, the values which were considered to be outside of the normal range were selected by using a cut-off. Besides Datum's correction, the deviated-wells were verified. At the same time a homogeneous isotropic medium, clastic reservoir and absence of radioactive sandstones were supposed.

This study was divided into two main phases. The initial phase (Phase 1) consisted mainly of the study of well logs in reservoirs, (reaching a thickness of 193.5ft from 2020.98ft to 2214.47ft), in which it was possible to identify the prospective area, fluid contacts, fluid types, 4 principal zones, as well as the performance of porosity estimation, hydrocarbon saturations and acoustic impedances. The second phase (Phase 2) consisted of fluid substitution using Gassmann's equation through an algorithm implemented in Matlab (see section 3.1.5). This took place in Zone 2, which exhibited a higher amount of oil saturation than in zones 1, 3 and 4. A profitable hydrocarbons quantity was not present in the aforementioned zones. An analysis of the most relevant results according to the previously mentioned phases will be explained below:

5.1 Analysis of the results (phase 1)

- The Caliper log showed a remarkable continuity in well geometry between zones 2 and 3 (with depths between 2042ft and 2150ft) showing slight variations in hole diameter. However, in zones 1 and 4 an abrupt change in continuity was observed. Also wash-out in the well walls were reported, specifically between the depths of 2150ft and 2170ft (see figure 16). However, irrelevant drilling mud invasions were observed. Such behaviour is due to current lithological differences, where landslides are related to a less competent lithology and lower compaction degree as Shales, the sandstones had a reasonably competent lithology, without the presence of landslides in the well walls.

- As far as the lithology is concerned, clastic sandstones were the most relevant rock type founded, and represent about 55% of the reservoir. The other 45% is distributed between thin layers of limestone and shale (See table 10).

- The identification of lithology was conducted using the Gamma Ray log in which the maximum ºAPI were Shales, characterized by high radioactivity, reaching values between 90 and 100 ºAPI (specifically in zones 1 and 4), while the clean sands presented an ºAPI between 20 and 30 (Zones 2 and 3), as shown in Figure 13.

- By integrating the results obtained from well logs, it was possible to divide the reservoir into 4 main areas, of which only zone 2 presented a set of representative characteristics of an oil reservoir. This can be seen in Table 8, where relevant information is reported about the 4 areas which were identified in this study. One of the most representative values observed is the water saturation average in zone 2 (48%). However in zone 3, that value was almost 90%. Zones 1 and 2 are irrelevant since they presented shale lithology. Furthermore, the porosities in zone 2 and 3 were between 12% and 13%. These porosities can contain profitable hydrocarbon.

- The fluids which were present in the reservoir were identified as brine and oil. They were recognized through the cross plot between the neutron and density logs, of which, the most relevant were identified to a depth of 2042ft and 2150ft (See figure 16). As it is known, a larger cross plot refers to gas, whereas a moderate cross plot refers to water or oil (according to the oil physical parameter the curve may be more or less pronounced). However, these indicators must be corroborated and compared with other logs such as resistivity and sonic logs, as well as water saturation quantities (See figure 17), in order to be able to have a more representative view about the present fluid properties.

- Certain patterns between deep resistivity and the density log were observed. They show a clear evidence of the presence of oil or water in the reservoir. Among the most relevant patterns a "Mae West" was observed between the depths of 2042ft – 2010ft, and a "Tramline" between 2100ft - 2150ft (See figure 16). This shows a clear sign of the presence of hydrocarbon and water respectively.

- The maximum and minimum values were crucial factors in order to identify the most prospective areas in the reservoir. The maximum value of resistivity was ohm.m 56.17, whereas the minimum value was 0.80 ohm.m. This represents resistivity values which are respectively related to oil and water.

- On the other hand, the minimum values of the Gamma Ray log are helpful in clastic reservoir lithology. This is because they act as a valuable lithology discriminate for the identification of clean sands (Figure 17). However, when performing the calculation of shale volume (Vsh) the maximum values of the Gamma Ray (between 91 and 114 º API) were not taken into account. This is due to the fact that these values are not representative of the reservoir.

- Through the interpolation of 8 samples with a pressure between 2047ft and 2171ft (See Table 5), it was possible to identify the pressure gradients 0.368 psia/ft and 0.440 psia/ft, which are respectively characteristic of an oil reservoir and an aquifer (See Table 6). Therefore, the oil water contact (WOC) was identified successfully at a depth of 2012ft, as it is shown in the figure 18. This value was supported by the density and resistivity logs, as well as through the calculated water saturations.

- The porosities obtained by the density log were approximately between 7% and 14% in both oil sands, and sands with high water saturations. In zone 2, these porosities were calibrated with samples (core porosity) to the same depth (See table 7). However, it is noteworthy that the porosities which were obtained by the density log were more representative than the porosities obtained through Neutron and Sonic logs. These showed some discrepancies with respect to the porosity of core porosity.

- With regards to water saturation, the maximum saturation zone was observed between the depths of 2150ft and 2120ft. However, between 2120ft and 2042ft, this proportion decreased significantly with values below 40%, while exhibiting water saturation values between 32% and 35%, and obtaining hydrocarbon saturation values between 60% and 78% (See table 8).

5.2 Analysis of the results (phase 2)

By using Gassmann's equation in Matlab, it was possible to perform fluid substitution, specifically in zone 2. An interpretation of the data obtained was performed before and after Gassmann's fluid substitution took place. The most relevant results will be discussed below:

- After the fluid substitution from Oil to Brine, changes in slight density were observed, which were between ± 3% compared to the initial values, as it is shown in the figure 24, and briefly summarized in table 11.

- As might be expected, when the oil was substituted for gas at different rates, (such as 50% and 95%), a significant decrease in the density was observed, between 2% and 12%. The minimum density values were observed where porosities are greater, as were the maximum density values where the porosities are smaller (See figures 22 and 23).

- After fluid substitution from Oil to brine fluids, significant changes in the behaviour of P waves velocities were observed. The P wave velocities increased in proportion from 2% to 18%, compared to its initial value. Meanwhile, the acoustic impedance (AI) showed a significant "peak" between the depths 2092ft and 2095ft (See figure 21). This corresponds to an increase of sound resistance, which is due to a change of interface between "sandstones" and "shale". This provides valuable lithological information in order to discriminate transitional interfaces.

- With regards to the S wave velocity, no significant changes in behaviour were reported (see equation 3). This is because the "Shear modulus" does not depend on the type of fluid in the pore space.

- With concern to fluid replacement from oil to gas, slight changes were observed in the behaviour of the P wave velocities, changing around ± 2% compared to its initial value. Meanwhile, the acoustic impedance (AI) showed a significant reduction, from 1% to 7% (See Table 11). This corresponds to a lower sound resistance, which is due to a decrease in density, which in turn is caused by the replacement of oil by gas.

6 Conclusions and recommendations

The thesis involves the data processing of borehole logs and the application of algorithm of Gassmann to analyse the response of a reservoir: the main results have pointed out:

- Through the analysis of borehole data, it was possible to successfully identify an oil reservoir, (located specifically in Zone 2) between the depths of 2120.47ft 2042.48ft. The reservoir presented a Net thickness of 70.5ft, with average porosities between 12 and 13%, (which are big enough to contain profitable amounts of hydrocarbon). Furthermore, this zone exhibited an excellent Oil saturation average of about 55%.

- The reservoir showed a significant percentage (about 55%) of clean sand, between depths of 2020.98ft - 2150.47ft. However, zone 2 presented a high quality lithology with 89% of oil sands characterized by being a competent lithology and composed primarily of quartz minerals.

- Through Gasmann's equation it was possible to successfully perform fluid replacement in oil (zone 2). This was implemented in Matlab through an explicit algorithm which evaluates multiple points according to the input.

- After the replacement of oil by brine took place, a slight increase in total densities of 0.5% was observed. However, a significant increase was reported with regards to acoustic impedance (AI), specifically between lithological interfaces as limestone-sandstone, and shale-sandstone, at a depth of 2050ft and 2095ft respectively.

- Regarding the replacement of oil fluids by gas, relevant changes in total densities were exhibited, decreasing to 4% with respect to the initial value. Meanwhile, the acoustic impedances (AI) also underwent changes, (decreasing to 2.5%) thus "masking" the response between sand-shale interfaces to a depth of 2095ft.

Recommendations:

The data interpretation could be improved by:

- Carry out an analysis of carbonate rocks in zones 2 and 4 in order to identify porosity and density variations, thereby optimizing the results.

- Perform a study of fluid substitution with respect to time, in order to compare variations and confirm the results before, during, and after well production. This could be accomplished in both zones 2 and 3.

- Calculate permeabilities using the "Poroperm relationship" into zones 2 and 3, in order to estimate important parameters like Mobility ratio (M), which gives us valuable information about the fluids behaviour, such as relating permeability to viscosity. Likewise, this parameter is an important input when performing a dynamic or static model.

7 Appendices

Appendix A: Compressional wave velocity for some fluids (J.H. Schön, 2011).

Fluid	VP in m s^{-1}	Remarks; Parameters
Air	263	T = 173ºK
	332	T = 273ºK
	387	T = 373ºK
Methane	488	p = 0.103 MPa
Carbon dioxide	259	
Oil; natural	1035-1370; mean 1280	
Paraffine oil	1420	T = 307 ºK; ρ= 835 kg m^{-3}
Gasoline oil	1250	T = 307ºK; ρ = 803 kg m^{-3}
Water	1497	T = 298ºK distilled
	1585	p = 0.103 MPa; 1000 ppm NaCl
	1638	p = 0.103 MPa; 1500 ppm NaCl
	1689	p = 0.103 MPa; 2000 ppm NaCl

Appendix B: Coefficients for water velocity computation (from Batzle and Wang, 1992).

$w_{11} = 1402.85$ $w_{13} = 3.437\times10^{-3}$

$w_{21} = 4.871$ $w_{23} = 1.739\times10^{-4}$

$w_{31} = -0.04783$ $w_{33} = -2.135\times10^{-6}$

$w_{41} = 1.487\times10^{-4}$ $w_{43} = -1.455\times10^{-8}$

$w_{51} = -2.197\times10^{-7}$ $w_{53} = 5.23\times10^{-11}$

$w_{12} = 1.524$ $w_{14} = -1.197\times10^{-5}$

$w_{22} = -0.0111$ $w_{24} = -1.628\times10^{-6}$

$w_{32} = 2.747\times10^{-4}$ $w_{34} = 1.237\times10^{-8}$

$w_{42} = -6.503\times10^{-7}$ $w_{44} = 1.327\times10^{-10}$

$w_{52} = 7.987\times10^{-10}$ $w_{54} = -4.614\times10^{-13}$

8 Bibliography

Batzle, M. L., and Wang, Z., 1992, Seismic properties of pore fluids: Geophysics, 64, 1396-1408.

Berryman, J. G., 1999, “Origin of Gassmann’s equation”: Geophysics, 64, 1627-1629.

Biot, 1956, Theory of propagation of elastic waves in a fluid saturated porous solid, 1. Low frequency range, J. Acoust. Soc. Am., 28, 179-191.

Bohlen T, Kugler S, Klein G and Theilen F: “Case History 1.5D Inversion of Lateral Variation of Scholte-Wave Dispersion,” Geophysics 69, no. 2 (March–April 2004): 330–344.

Brian H. Russell et al, 2001, “Fluid-property discrimination with AVO: A Biot-Gassmann perspective”, volume 3, 403-419.

Dewar J. and Pickford S., 2001. Rock physics for the Rest of US-An Informal Discussion. A Core Laboratory Company.

Djebbar Tiab & Erle C. Donaldson, 2012, Petrophysics, Theory and Practice of Measuring Reservoir Rock and Fluid Transport Properties Third edition, chapter 85 – 215.

Gassmann Fritz, 1951,"On Elasticity of Porous Media", Zurich, Switzerland, version date: January 9, 1998.

Hill, R., 1952, The elastic behavior of a crystalline aggregate: Proc. Phys. Soc. London Ser. A, 65, 349-354.

Jakob B.U. Haldorsen, David Linton Johnson, Tom Plona, Bikash Sinha, Henri-Pierre Valero, Kenneth Winkler, Spring 2006. Borehole Acoustic Waves, Ridgefield, Connecticut, USA 34 – 43.

Kumar Dhananjay, 2006, Tutorial on Gassmann Fluid Substitution: Formulation, Algorithm and Matlab Code, Chevron Energy Technology Company, California.

Leiv J. 2007, “Introduction to seismic processing and imaging”, Gelius GeoCLASS. The University of Oslo, Norwegian.

Mavko, G., Mukerji, T., and Dvorkin, J., 1998, The rock physics handbook: Tools for seismic analysis in porous media: Cambridge Univ. Press.

Nawras Al-Khateb, 2013, CHORUS Heavy Oil Consortium, Department of Geoscience, University of Calgary.

Schon, 2011, Physical Properties of Rocks: A workbook, J.H., chapter 6, 149 – 155.

Toby Darling, 2005, Gulf drilling guides, well logging and formations evaluation, Oxford OX2 8DP, UK.

Wang, Z. (2001). Y2K tutorial: Fundamentals of seismic rock physics.Geophysics, 66, pp. 398–412.

Zhu, X., and McMechan, G. A., 1990, Direct estimation of the bulk modulus of the frame in fluid saturated elastic medium by Biot theory: 60th Ann. Internat. Mtg., Soc. Expl. Geophys., Expanded Abstract, 787-790.